

Resonance near Border-Collision Bifurcations in Piecewise-Smooth, Continuous Maps.

D.J.W. Simpson[†] and J.D. Meiss^{‡*}

[†]Department of Mathematics
University of British Columbia
Vancouver, BC, V6T1Z2
Canada

[‡]Department of Applied Mathematics
University of Colorado
Boulder, CO, 80309-0526
USA

October 30, 2018

Abstract

Mode-locking regions (resonance tongues) formed by border-collision bifurcations of piecewise-smooth, continuous maps commonly exhibit a distinctive sausage-like geometry with pinch points called “shrinking points”. In this paper we extend our unfolding of the piecewise-linear case [*Nonlinearity*, 22(5):1123-1144, 2009] to show how shrinking points are destroyed by nonlinearity. We obtain a codimension-three unfolding of this shrinking point bifurcation for N -dimensional maps. We show that the destruction of the shrinking points generically occurs by the creation of a curve of saddle-node bifurcations that smooth one boundary of the sausage, leaving a kink in the other boundary.

1 Introduction

Piecewise-smooth systems are used to model a vast range of physical systems involving nonsmooth behavior [1, 2, 3, 4]. In this paper we study piecewise-smooth, continuous maps, i.e.

$$x_{i+1} = F(x_i) , \quad (1)$$

*DJWS acknowledges support from an NSERC Discovery Grant. JDM acknowledges support from NSF grant DMS-0707659.

where $x_i \in \mathbb{R}^N$ and F is everywhere continuous but nondifferentiable on codimension-one surfaces in \mathbb{R}^N called *switching manifolds*. Such maps arise as Poincaré maps of Filippov systems near grazing-sliding and corner collisions [5, 6] or of some time-dependent piecewise-smooth flows [7]. They are often used as mathematical models of various discrete, nonsmooth systems, see e.g. [8].

A fundamental and unique bifurcation of piecewise-smooth, continuous maps results from the collision of a fixed point with a switching manifold; it is known as a *border-collision bifurcation*. Except in degenerate cases, a border-collision bifurcation may be classified as either a *border-collision fold* at which two fixed points collide and annihilate, or a *border-collision persistence* at which a single fixed point “crosses” the switching manifold [1, 9]. Note that the collision of one point of a periodic solution of (1) with a switching manifold is also a border-collision bifurcation for the n^{th} iterate of (1) [9, 10]. Though complicated dynamics may be born in border-collision bifurcations, in this paper we study only the creation of periodic solutions.

We assume that the derivatives of the smooth components of (1), $D_x F$, are locally bounded (we exclude from consideration, for instance, square-root type maps [1, 11]). Then, generic border-collision bifurcations of (1) may be described by piecewise-linear maps. More precisely, structurally-stable dynamics of a piecewise-smooth, continuous map near a border-collision bifurcation are described by the piecewise-linear, series expansion about the bifurcation. A consequence is that, to lowest order, the structurally-stable invariant sets created at border-collision bifurcations grow linearly as the bifurcation parameter varies.

One example is the two-dimensional, piecewise-smooth, continuous map

$$f_\mu(x) = \begin{cases} \mu \begin{bmatrix} 1 \\ 0 \end{bmatrix} + \begin{bmatrix} 2r_L \cos(2\pi\omega_L) & 1 \\ -r_L^2 & 0 \end{bmatrix} x + g^L(x), & s \leq 0 \\ \mu \begin{bmatrix} 1 \\ 0 \end{bmatrix} + \begin{bmatrix} \frac{2}{s_R} \cos(2\pi\omega_R) & 1 \\ -\frac{1}{s_R^2} & 0 \end{bmatrix} x + g^R(x), & s \geq 0 \end{cases}, \quad (2)$$

where

$$s \equiv e_1^\top x \quad (\text{the first component of the vector } x \in \mathbb{R}^2),$$

$0 < r_L, s_R < 1$, $0 < \omega_L, \omega_R < \frac{1}{2}$, $\mu \in \mathbb{R}$ is assumed to be small, and the functions $g^L(x)$ and $g^R(x)$ contain the terms of f_μ that are nonlinear in x . The map (2) is continuous only if $g^L(x) = g^R(x)$ whenever $s = 0$, i.e., on the switching manifold.

A border-collision bifurcation for (2) occurs at the origin when $\mu = 0$. If this bifurcation is nondegenerate, the local dynamics are independent of the nonlinear components, g^L and g^R .

The piecewise-linear version of (2), i.e., with

$$g^L(x) = g^R(x) = \begin{bmatrix} 0 \\ 0 \end{bmatrix}, \quad (3)$$

is the canonical, piecewise-linear form for a border-collision analogue to a smooth Neimark-Sacker bifurcation. Indeed the fixed point for $\mu < 0$ has a pair of complex multipliers ($\lambda_\pm = r_L e^{\pm 2\pi i \omega_L}$) inside the unit circle that “jump” at $\mu = 0$ outside the unit circle ($\lambda_\pm =$

$\frac{1}{s_R}e^{\pm 2\pi i\omega_R}$) for $\mu > 0$. Depending upon the precise choice of parameter values, this border-collision bifurcation may generate periodic, quasiperiodic, or chaotic solutions as well as combinations of these [12, 13, 14, 15]. This class of border-collision bifurcations has been seen in models of DC/DC power converters [7] and optimization in economics [8, 16].

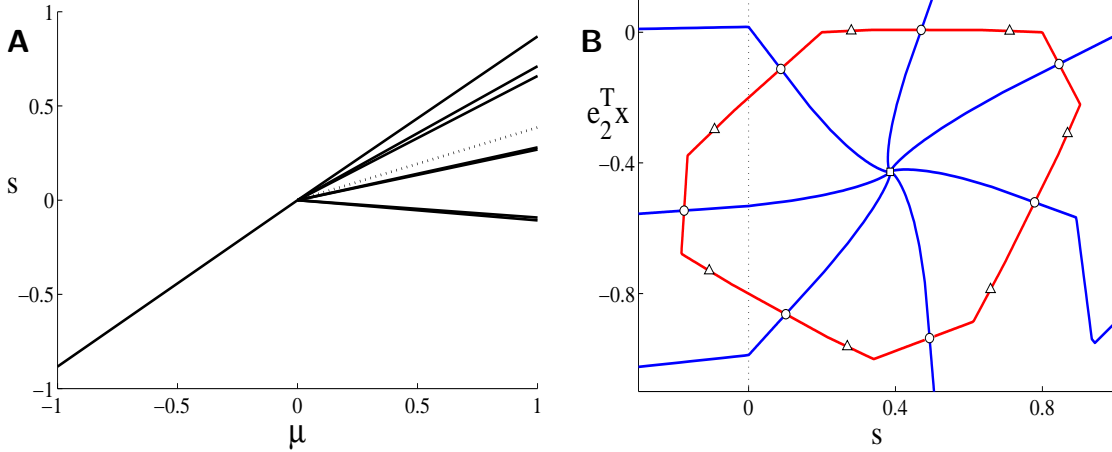


Figure 1: Panel A shows a bifurcation diagram of (2) with (3) when $r_L = 0.2$, $s_R = 0.95$ and $\omega_L = \omega_R = 0.287$. When $\mu < 0$ the unique fixed point is attracting (the solid line) and when $\mu > 0$ it is repelling (the dotted line) and a pair of period-seven orbits exist. The solid lines for $\mu > 0$ in panel A show the attracting 7-cycle (two pairs of points have similar s -values). Panel B shows a phase portrait when $\mu = 1$. The dotted vertical line is the switching manifold. The attracting [saddle] 7-cycle is indicated by triangles [circles]. The unstable manifold of the saddle forms an invariant circle (red); the curves forming its stable manifold (blue) intersect at the repelling fixed point (square).

Fig. 1-A shows an example of a bifurcation diagram for (2) with (3) when a pair of period-seven orbits (7-cycles) is created at $\mu = 0$. These two orbits are shown in panel B; one is attracting and the other is a saddle. The unstable manifold of the saddle forms an invariant circle that contains the attracting orbit. This border-collision bifurcation is nondegenerate; indeed, if we were to relax (3) then there is an $\varepsilon > 0$ such that whenever $0 < \mu < \varepsilon$ the dynamics are topologically equivalent to Fig. 1-B near the origin. An example is shown in Fig. 2 where

$$g^L(x) = \begin{bmatrix} s^2 \\ 0 \end{bmatrix} \quad g^R(x) = \begin{bmatrix} 0 \\ 0 \end{bmatrix}. \quad (4)$$

For this nonlinear system, there is also a saddle-node pair of period-seven orbits created at the border-collision bifurcation. The stable 7-cycle is attracting up to $\mu \approx 1.202$.

Note that piecewise-linear maps are particularly straightforward to analyze because any periodic orbit is the solution to a linear system. Furthermore, linearity implies that if \mathcal{I} is an invariant set of f_μ then $\lambda\mathcal{I}$ is an invariant set of $f_{\lambda\mu}$ for any $\lambda > 0$. Consequently it suffices to consider $\mu = -1, 0, 1$.

A two-parameter bifurcation diagram of the piecewise-linear case of (2) is shown in Fig. 3 for $\mu = 1$. The colored regions are resonance (or Arnold) tongues within which there is an

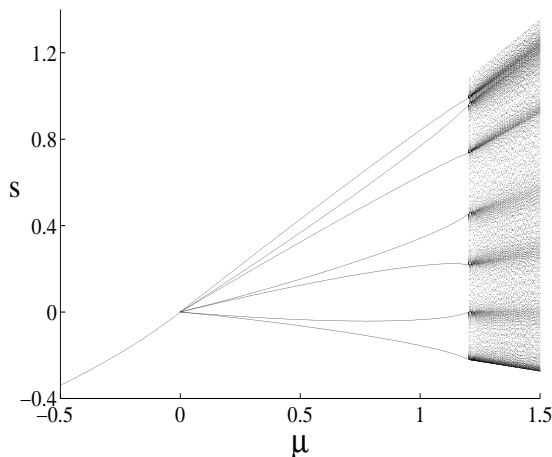


Figure 2: A bifurcation diagram showing attracting orbits of (2) with nonlinearity (4) at the same parameter values in Fig. 1. When μ is small the dynamical behavior near the origin is topologically equivalent to the linear case. However, at $\mu \approx 1.202$, the attracting 7-cycle undergoes border-collision beyond which there exists a complicated attracting set.

attracting periodic solution. Since the piecewise-linear case of the two-dimensional map (2) has a unique fixed point, we may define a rotation number for orbits as the average change in angle per iteration about the fixed point [12, 17, 18, 19]. Consequently the resonance tongues can be labeled by the rotation number, m/n , of the corresponding periodic solution. The orbits shown in Fig. 1 lie in the $2/7$ -tongue; this tongue intersects the $s_R = 1$ line at $\omega_R = 2/7 \approx 0.2857$.

The majority of the resonance tongues in Fig. 3 exhibit a structure that is often likened to a string of sausages. This structure was first observed in a one-dimensional sawtooth map [21], and has since been described in higher dimensional maps such as (2), see for example [14, 7, 22, 8, 16]. As in [21], we refer to points where resonance tongues have zero width as *shrinking points*¹.

An unfolding of shrinking points in piecewise-linear, continuous maps of arbitrary dimension was performed in [10]. There it was shown, upon imposing reasonable nondegeneracy assumptions, that any two-dimensional slice of parameter space in the neighborhood of a shrinking point will resemble Fig. 4: shrinking points are codimension-two phenomena of piecewise-linear, continuous maps. In particular, near a shrinking point, the resonance tongue is locally a two-dimensional cone bounded by four curves. These boundary curves are pairwise tangent at the shrinking point so the cone boundaries are locally C^1 . In the interior of the cone a *primary n -cycle* exists; it has some number of points, say l , located, “left”, of the switching manifold ($l = 2$ for Fig. 4). This orbit collides and annihilates with another n -cycle in a border-collision fold bifurcation on the four boundary curves of the cone. This secondary periodic solution has $l - 1$ points to the left of the switching manifold within one half of the cone and $l + 1$ points to the left of the switching manifold within the other half

¹In this paper we will only consider the case of “non-terminating” shrinking points defined in [10]. Thus we do not consider the ends of resonance tongues such as those at $s_R = 1$ in Fig. 3.

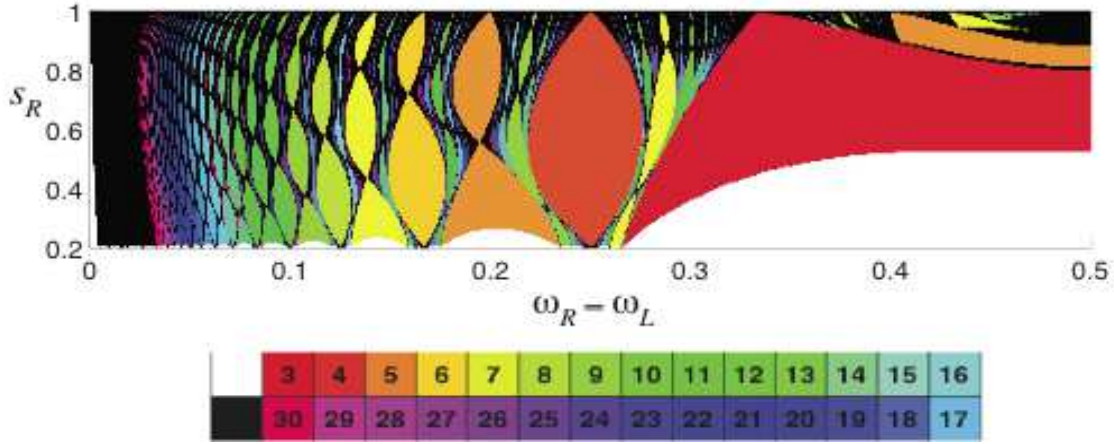


Figure 3: Resonance tongues of (2) with (3) for $r_L = 0.2$ and $\mu = 1$. Each colored region corresponds to the existence of a periodic solution with period indicated in the color bar. The rotation number in each resonance tongue is equal to the value of ω_R at which it emanates from the line, $s_R = 1$. White regions correspond to no observed attractor; black regions correspond to the existence of a bounded forward orbit that is either aperiodic or has period larger than 30. Similar figures at different parameter values are given in [12, 20].

of the cone. On each of the four boundary curves a different point of the primary orbit lies on the switching manifold.

These results generalize to the nonlinear case in the following sense: regardless of the nonlinearities g^L and g^R , the two-dimensional bifurcation structure shown in Fig. 3 will be essentially unchanged when μ is small enough and it will limit to the linear picture as $\mu \rightarrow 0^+$. However, when nonlinear terms are present the sausage structure is not preserved as μ increases; indeed, the shrinking points break apart as shown in Fig. 5. Consequently when nonlinear terms are present the phenomenon is codimension-three; we refer this scenario as a *generalized shrinking point*.

Fig. 5 suggests that the break-up of shrinking points occurs in a regular fashion. The resonance tongues develop a nonzero width that increases with μ . For $\mu > 0$ the right boundary of each resonance tongue appears to be smooth whereas each left boundary retains the kink that appeared at the shrinking point. It is interesting that, in contrast to the case for smooth maps, we observe no “strong” resonance behavior when $n < 5$.

The purpose of this paper is to determine the generic unfolding of generalized shrinking points for a piecewise-smooth, continuous map of arbitrary dimension. Here we summarize our results. Suppose that a border-collision bifurcation occurs when a parameter μ is zero, that resonance arises for $\mu > 0$, and that in the limit $\mu \rightarrow 0^+$, a two-parameter bifurcation diagram exhibits a shrinking point with its four boundary curves. For small $\mu > 0$ the four boundary curves maintain a common intersection point, O , but each curve is no longer necessarily tangent to the opposite curve at this point.

We will show that, under reasonable nondegeneracy assumptions, there exists a new bifurcation locus for each small enough fixed $\mu > 0$. This locus is a curve of saddle-node

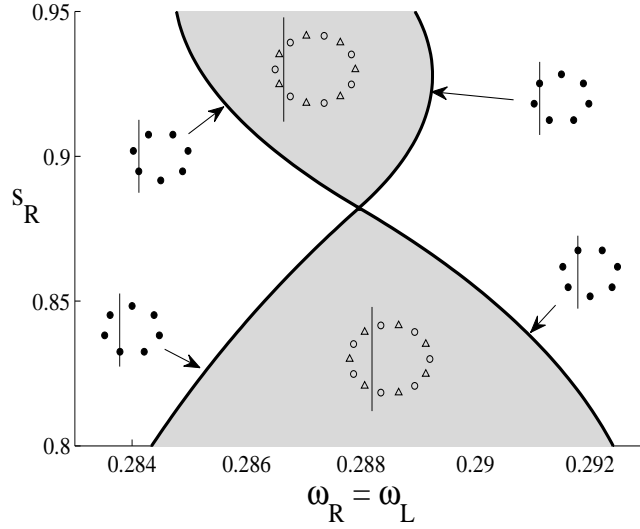


Figure 4: A magnification of the $2/7$ resonance tongue in Fig. 3 near a shrinking point. Orbits that exist in the resonance tongue are shown in inserted phase portraits (not to scale) as the open circles and triangles. Above the shrinking point, these have $l = 1$ and $l = 2$ (l represents the number of points that lie left of the switching manifold) and below the shrinking point, $l = 2$ and $l = 3$. On the four boundary curves the two coexisting periodic solutions collide and annihilate in border-collision fold bifurcations. On each of the four boundary curves a different point of the primary orbit (with $l = 2$), lies on the switching manifold. These orbits are sketched in phase portraits with filled circles. Compare this to panel B of Fig. 1, an actual phase portrait at $(\omega_R, s_R) = (0.287, 0.95)$.

bifurcations of the primary n -cycle that is tangent to one boundary curve at a point A , and to an adjacent boundary curve on the other side of the shrinking point at B , see Fig. 6. This locus is smooth and collapses to the shrinking point as $\mu \rightarrow 0^+$. Two n -cycles that have the same itinerary as the primary n -cycle exist in a triangular region bounded by O , A and B . If we let θ_1 denote the angle made at O between the two border-collision curves across the region AOB , see Fig. 6, and θ_2 is the opposing angle made at O between the other two border-collision curves, then for small $\mu > 0$, $\theta_1 < \theta_2$.

A formal statement that includes these results is given in Thm. 10 in §6.

Here we summarize the remainder of the paper. In the following section we present the N -dimensional map (6) that describes an arbitrary border-collision bifurcation. Concepts from symbolic dynamics that are invaluable for describing periodic solutions of (6) are introduced in §3. Key formulas for periodic solutions are obtained in §4. Subsequently we impose the assumption that (6) is piecewise- C^K ; this allows us to derive useful series expansions. Section 5 is devoted to defining generalized shrinking points as a codimension-three scenario. Finally in §6 we unfold these points leading to Thm. 10. The proofs of the theorem and Lemma 9 are given in an appendix.

Throughout the paper we use $O(k)$ [$o(k)$] to denote terms that are order k or larger [larger than order k] in all variables and parameters of a given expression.

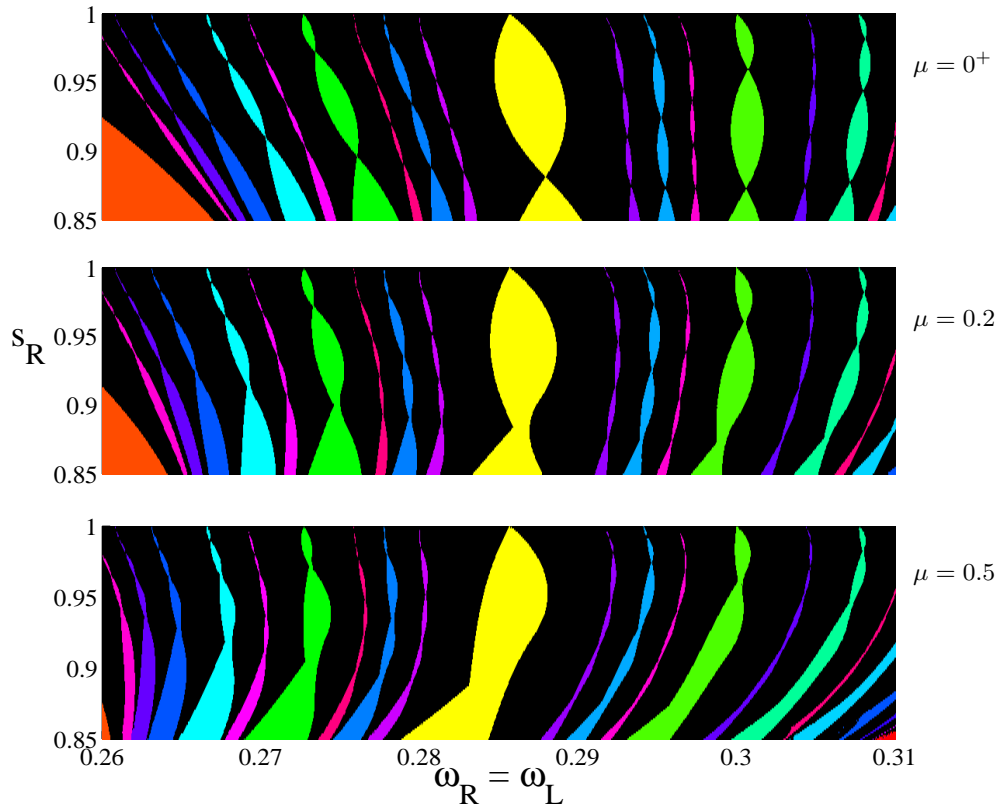


Figure 5: Resonance tongues of (2) with (4) when $r_L = 0.2$ for three different values of μ . The uppermost plot is a magnification of Fig. 3. The lower two plots were computed numerically by estimating the eventual period of the forward orbit of the origin.

2 Generic border-collision bifurcations

We restrict our attention to local dynamics of border-collision bifurcations, and thus study a piecewise-smooth series expansion of (1) about an arbitrary border-collision bifurcation. Throughout this paper we will assume that there is a single, smooth switching manifold in a neighborhood of the border-collision bifurcation. This is typically the case in models since switching manifolds are usually defined by some simple physical constraint. For simplicity we assume that a coordinate transformation has been made so that the switching manifold corresponds to the vanishing of the first component of x (see in particular [23] for details of such a transformation) and—to avoid the use of subscripts for components—we introduce the new variable

$$s = e_1^\top x. \quad (5)$$

A general piecewise-smooth map then takes the form

$$x_{i+1} = f(x_i; \xi) = \begin{cases} f^L(x_i; \xi), & s_i \leq 0 \\ f^R(x_i; \xi), & s_i \geq 0 \end{cases}, \quad (6)$$

where ξ is a vector of parameters. The switching manifold partitions phase space into two regions: the *left half-space* (where $s < 0$) and the *right half-space* (where $s > 0$).

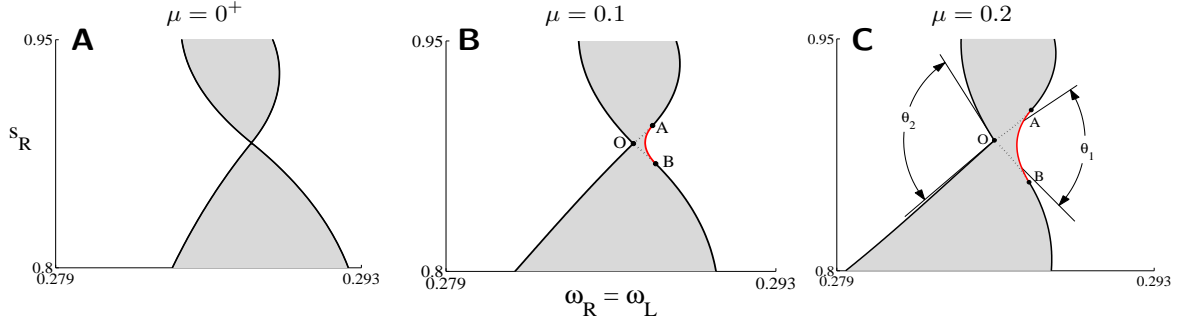


Figure 6: Bifurcation sets of (2) with (4) for $r_L = 0.2$ and three different μ values. Panel A is identical to Fig. 4. In panels B and C the locus of classical saddle-node bifurcations of the primary orbit is indicated by a red curve. Solid [dotted] curves correspond to border-collision fold bifurcations [border-collision persistence].

We assume a border-collision bifurcation of a fixed point occurs at the origin when a parameter μ is zero so that the functions f^L and f^R have series expansions

$$f^J(x_i; \xi) = \mu b(\xi) + A_J(\xi)x_i + g^J(x_i; \xi), \quad (7)$$

where $J = L, R$, μ is the first component the parameters ξ , A_J is an $N \times N$ matrix, $b \in \mathbb{R}^N$. The functions g^J contain only terms that are nonlinear in x ; that is, $g^J(x_i; \xi) = o(|x_i|)$ (this, for example, could include terms of order $|x_i|^{\frac{3}{2}}$ that arise naturally in Poincaré maps relating to sliding bifurcations). By continuity of (6), A_L and A_R are identical in their last $N - 1$ columns and $g^L = g^R$ whenever $s = 0$.

If $A_J(\xi)$ does not have an eigenvalue 1, the half-map f^J has a unique fixed point near the origin given explicitly by

$$x^{*J}(\xi) = (I - A_J(\xi))^{-1}b(\xi) \Big|_{\mu=0} \mu + o(\mu). \quad (8)$$

As seems to have been first noted by Feigin, see [9], a convenient expression for the first component of the vector, x^{*J} , is obtained with adjugate matrices [24, 25]:

$$\text{adj}(X)X = \det(X)I, \quad \text{for any } N \times N \text{ matrix } X. \quad (9)$$

The point is that since A_L and A_R are identical in their last $N - 1$ columns, $\text{adj}(I - A_L)$ and $\text{adj}(I - A_R)$ share the same first row:

$$\varrho^T(\xi) = e_1^T \text{adj}(I - A_L(\xi)) = e_1^T \text{adj}(I - A_R(\xi)). \quad (10)$$

Consequently, multiplication of (8) by e_1^T on the left implies that the first component of the fixed point x^{*J} satisfies the useful formula

$$s^{*J}(\xi) = \frac{\varrho^T(\xi)b(\xi)}{\det(I - A_J(\xi))} \Big|_{\mu=0} \mu + o(\mu). \quad (11)$$

In particular we learn from (11) that both fixed points, if they exist, move away from the switching manifold linearly with respect to μ if and only if $\varrho^\top(\xi)b(\xi)|_{\mu=0} \neq 0$. This condition is a nondegeneracy condition for the border-collision bifurcation. Under this assumption, the bifurcation is a border-collision fold bifurcation if $\det(I - A_L(0))$ and $\det(I - A_R(0))$ have opposite signs, and border-collision persistence if they have the same sign [9].

3 Symbolic dynamics

It is common in the study of piecewise-smooth systems for symbolic methods to be highly beneficial. In this paper we consider bi-infinite sequences, \mathcal{S} , constructed from the binary alphabet $\{\mathbf{L}, \mathbf{R}\}$. In order to unfold shrinking points, we find it necessary to consider only what we have termed *rotational symbol sequences*. In [10] we defined these as particular finite collections. Instead of repeating this definition we provide here a definition that is more versatile in that it extends naturally to nonperiodic sequences and has been described elsewhere. Furthermore, to be consistent with combinatorics literature sequences are always assumed to contain infinitely many elements (unlike in [10]).

Definition 1. For $\alpha, \beta \in [0, 1)$, let $\mathcal{S}[\alpha, \beta]$, be the bi-infinite symbol sequence with i^{th} element

$$\mathcal{S}[\alpha, \beta]_i \equiv \begin{cases} \mathbf{L}, & i\alpha \bmod 1 \in [0, \beta) \\ \mathbf{R}, & i\alpha \bmod 1 \in [\beta, 1) \end{cases}, \text{ for all } i \in \mathbb{Z}.$$

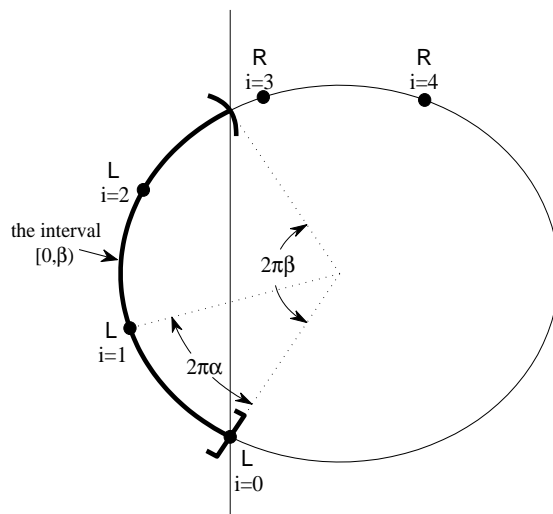


Figure 7: A geometric portrayal of Def. 1. First cut a circle with a vertical line that subtends an angle $2\pi\beta$ as shown. Each real number, ϕ , is then represented by a point $2\pi\phi$ radians clockwise from the lower intersection of the circle with the vertical line. Then $\mathcal{S}_i[\alpha, \beta] = \mathbf{L}$ whenever $\phi = i\alpha$ is located to the left of the vertical line, and $\mathcal{S}_i[\alpha, \beta] = \mathbf{R}$ otherwise. In addition $\mathcal{S}_0[\alpha, \beta]$ is always \mathbf{L} .

A visual representation of these sequences is provided by Fig. 7. These sequences seem to have first been studied by Slater [26, 27]. The sequences for which $\alpha = \beta \notin \mathbb{Q}$ have been well studied and are known as *rotation sequences*; they are equivalent to *Sturmian sequences* [28], which are traditionally defined from a combinatorics viewpoint [29]. Some discussion of the case $\alpha = \beta \in \mathbb{Q}$ is given in [30]. A related approach is to consider arithmetic sequences on $\mathbb{Z}/n\mathbb{Z}$ for some $n \in \mathbb{N}$ [31]. Similar sequences for rotational orbits of the Hénon map are described in [32].

Definition 2 (Rotational Symbol Sequence). For each $l, m, n \in \mathbb{N}$ with $l, m < n$ and $\gcd(m, n) = 1$, $\mathcal{S}[\frac{m}{n}, \frac{l}{n}]$ is a *rotational symbol sequence*.

Any periodic sequence, such as $\mathcal{S}[\frac{m}{n}, \frac{l}{n}]$, is generated by repeated copies of a finite collection from $\{L, R\}$, termed a *word*. For instance for the word $\mathcal{W} = \text{LLR}$, the generated sequence is $\mathcal{S} = \dots \text{LLRLLRLLR} \dots$. Here we let $\mathcal{W}[l, m, n]$ denote the word comprised of the $i = 0, 1, \dots, n-1$ elements of $\mathcal{S}[\frac{m}{n}, \frac{l}{n}]$.

As an example, let us compute $\mathcal{S}[\frac{2}{7}, \frac{3}{7}]$. Here $\alpha = \frac{2}{7}$, thus the numbers $i\alpha \bmod 1$ of Def. 1 for $i = 0, 1, \dots, n-1$ are $0, \frac{2}{7}, \frac{4}{7}, \frac{6}{7}, \frac{1}{7}, \frac{3}{7}, \frac{5}{7}$, and $\beta = \frac{3}{7}$, therefore $\mathcal{W}[3, 2, 7] = \text{LLRRLRR}$.

Throughout this paper we will use the symbol d to denote the multiplicative inverse of m modulo n , for example $d = 4$ when $m = 2$ and $n = 7$ as above. Then

$$\mathcal{W}[l, m, n]_{id} = \begin{cases} L, & i = 0, \dots, l-1 \\ R, & i = l, \dots, n-1 \end{cases}, \quad (12)$$

where id is taken modulo n . For clarity, throughout this paper we omit “mod n ” where it is clear modulo arithmetic is being used.

Given a word \mathcal{W} , we let $\mathcal{W}^{(i)}$ denote the i^{th} left cyclic permutation of \mathcal{W} and $\mathcal{W}^{\bar{i}}$ denote the word that differs from \mathcal{W} in only the i^{th} element. For example if $\mathcal{W} = \text{LRLRR}$ then $\mathcal{W}^{\bar{3}} = \text{LRLLR}$ and $\mathcal{W}^{(2)} = \text{LRRLR}$. If \mathcal{S} is the sequence generated by \mathcal{W} we let $\mathcal{S}^{(i)}$ and $\mathcal{S}^{\bar{i}}$ denote the sequences generated by $\mathcal{W}^{(i)}$ and $\mathcal{W}^{\bar{i}}$, respectively.

A key property of symbol sequences that is verified in [10] is

$$\mathcal{S}[\frac{m}{n}, \frac{l}{n}]^{((l-1)d)\bar{0}} = \mathcal{S}[\frac{m}{n}, \frac{l}{n}]^{\bar{0}(ld)}. \quad (13)$$

4 Periodic solutions

For any symbol sequence \mathcal{S} , the iterates of a point $x_0 \in \mathbb{R}^N$ under the two half-maps of (6) in the order determined by \mathcal{S} are

$$x_{i+1} = f^{(S_i)}(x_i; \xi) \quad (14)$$

In general this may be different from iterating x_0 under the map (6). However, if the sequence $\{x_i\}$ satisfies the *admissibility condition*:

$$\mathcal{S}_i = \begin{cases} L, & \text{whenever } s_i < 0 \\ R, & \text{whenever } s_i > 0 \end{cases} \quad (15)$$

for every i , then $\{x_i\}$ coincides with the orbit of x_0 under (6). Notice if $s_i = 0$ there is no restriction on \mathcal{S}_i . When (15) holds for every i , $\{x_i\}$ is admissible, otherwise it is virtual.

When \mathcal{S} has period n , the periodic orbits with this sequence are admissible fixed points of the map

$$f^{\mathcal{S}} = f^{\mathcal{S}_{n-1}} \circ \dots \circ f^{\mathcal{S}_0} . \quad (16)$$

Some straightforward algebra leads to

$$f^{\mathcal{S}}(x; \xi) = P_{\mathcal{S}}(\xi) b(\xi) \Big|_{\mu=0} \mu + o(\mu) + \left(M_{\mathcal{S}}(\xi) \Big|_{\mu=0} + o(\mu^0) \right) x + o(x) , \quad (17)$$

where

$$M_{\mathcal{S}} = A_{\mathcal{S}_{n-1}} \dots A_{\mathcal{S}_0} , \quad (18)$$

$$P_{\mathcal{S}} = I + A_{\mathcal{S}_{n-1}} + A_{\mathcal{S}_{n-1}} A_{\mathcal{S}_{n-2}} + \dots + A_{\mathcal{S}_{n-1}} \dots A_{\mathcal{S}_1} . \quad (19)$$

Notice $P_{\mathcal{S}}$ is independent of \mathcal{S}_0 , thus

$$P_{\mathcal{S}} = P_{\mathcal{S}^{\bar{0}}} . \quad (20)$$

We now present six lemmas relating to periodic solutions that are useful for analyzing shrinking points. A consequence of the following lemma is that $M_{\mathcal{S}}$ and $M_{\mathcal{S}^{\bar{0}}}$ are identical in their last $N - 1$ columns.

Lemma 1. *For any $N \times N$ matrix, X , $XA_{\mathbf{R}} = XA_{\mathbf{L}} + \zeta e_1^{\top}$, for some $\zeta \in \mathbb{R}^N$.*

Proof. Since $A_{\mathbf{L}}$ and $A_{\mathbf{R}}$ are identical in all but possibly their first columns, we may write $A_{\mathbf{R}} = A_{\mathbf{L}} + \hat{\zeta} e_1^{\top}$ for some $\hat{\zeta} \in \mathbb{R}^N$. This proves the result with $\zeta = X\hat{\zeta}$. \square

If x_0 is a fixed point of $f^{\mathcal{S}}$ then the n points $\{x_0, \dots, x_{n-1}\}$ (where x_i is defined by (14)) describe a periodic solution (which may be virtual) that we will refer to as an \mathcal{S} -cycle. The following two lemmas are generalizations of those given in [10].

Lemma 2. *Suppose $\{x_i\}$ is an \mathcal{S} -cycle and x_j lies on the switching manifold, for some j . Then $\{x_i\}$ is also an $\mathcal{S}^{\bar{j}}$ -cycle.*

Proof. By continuity: $f^{\mathbf{L}}(x_j; \xi) = f^{\mathbf{R}}(x_j; \xi)$, hence there is no restriction on the j^{th} element of \mathcal{S} . \square

Lemma 3. *Suppose $\{x_i\}$ is an \mathcal{S} -cycle. Then for any j , $\det(I - D_x f^{\mathcal{S}^{(j)}}(x_j; \xi)) = \det(I - D_x f^{\mathcal{S}}(x_0; \xi))$.*

Proof. By the chain rule the Jacobian $D_x f^{\mathcal{S}}(x_0; \xi)$ may be written as a product of matrices:

$$D_x f^{\mathcal{S}}(x_0; \xi) = \prod_{i=n-1}^0 D_x f^{\mathcal{S}_i}(x_i; \xi) .$$

The spectrum of this product is unchanged if the N matrices are multiplied in an order that differs only cyclically from this one (refer to the proof of Lemma 4 of [10]), which proves the result. \square

Whenever $M_S(\xi)$ does not have an eigenvalue 1, the implicit function theorem implies that f^S has a unique fixed point near the origin, call it x^{*S} . Using (17) we obtain

$$x^{*S}(\xi) = (I - M_S(\xi))^{-1} P_S(\xi) b(\xi) \Big|_{\mu=0} \mu + o(\mu) . \quad (21)$$

We may derive a formula for the first component of x^{*S} , denoted s^{*S} , in the same spirit as (11) for fixed points of (6). Let

$$\varrho_S^T(\xi) = e_1^T \text{adj}(I - M_S(\xi)) , \quad (22)$$

then

$$s^{*S}(\xi) = \frac{\varrho_S^T(\xi) P_S(\xi) b(\xi)}{\det(I - M_S(\xi))} \Big|_{\mu=0} \mu + o(\mu) . \quad (23)$$

As in [20] we use two lemmas to derive a convenient formula for s^{*S} .

Lemma 4. *The matrices $P_S(I - A_{S_0})$ and $I - M_S$ can differ in only their first columns.*

Proof. Using (18) and (19),

$$\begin{aligned} P_S(I - A_{S_0}) &= (I + A_{S_{n-1}} + A_{S_{n-1}} A_{S_{n-2}} + \cdots + A_{S_{n-1}} \cdots A_{S_1})(I - A_{S_0}) \\ &\quad \text{expand and group terms differently:} \\ &= I - M_S + (A_{S_{n-1}} - A_{S_0}) + A_{S_{n-1}}(A_{S_{n-2}} - A_{S_0}) + \cdots \\ &\quad \quad \quad + A_{S_{n-1}} \cdots A_{S_2}(A_{S_1} - A_{S_0}) \\ &\quad \text{apply Lemma 1:} \\ &= I - M_S + \zeta_{n-1} e_1^T + \zeta_{n-2} e_1^T + \cdots + \zeta_1 e_1^T \\ &\quad \text{where each } \zeta_i \in \mathbb{R}^N, \\ &= I - M_S + \left(\sum_{i=1}^{n-1} \zeta_i \right) e_1^T . \end{aligned}$$

□

Lemma 5. $\varrho_S^T P_S = \det(P_S) \varrho^T$, where ϱ_S^T is given by (22) and ϱ^T is given by (10).

Proof. By Lemma 4 we have

$$\begin{aligned} e_1^T \text{adj}(P_S(I - A_{S_0})) &= e_1^T \text{adj}(I - M_S) = \varrho_S^T \\ \Rightarrow e_1^T \text{adj}(I - A_{S_0}) \text{adj}(P_S) &= \varrho_S^T \quad (\text{since } \text{adj}(XY) = \text{adj}(Y) \text{adj}(X) \text{ for any } X, Y) \\ \Rightarrow \varrho^T \text{adj}(P_S) &= \varrho_S^T \quad \text{by (10)} \\ \Rightarrow \det(P_S) \varrho^T &= \varrho_S^T P_S \quad \text{by (9)} \end{aligned}$$

□

If $I - M_{\mathcal{S}}(\xi)$ is nonsingular, by Lemma 5 and (23),

$$s^{*\mathcal{S}}(\xi) = \frac{\det(P_{\mathcal{S}}(\xi))}{\det(I - M_{\mathcal{S}}(\xi))} \varrho^{\mathsf{T}}(\xi) b(\xi) \Big|_{\mu=0} \mu + o(\mu) . \quad (24)$$

This expression relates the linear component of $s^{*\mathcal{S}}(\xi)$ simply in terms of $\varrho^{\mathsf{T}} b$ (which appears in the fixed point equation (11)) and the determinants of $P_{\mathcal{S}}$ and $I - M_{\mathcal{S}}$. (Feigin's result concerning the creation of 2-cycles at border-collision bifurcations (see [9]) follows from (24) by substituting $\mathcal{S} = \text{LR}$ and $\mathcal{S} = \text{RL}$).

We finish this section with an important lemma that is most simply stated for (6) in the absence of nonlinear terms, for then all $o(\mu)$ terms given above vanish. Though this result is proved in [10], with the use of Lemma 5 we are now able to provide a pithier proof.

Lemma 6. *Suppose the map (6) is piecewise-linear, that is $g^{\text{L}} = g^{\text{R}} = 0$, and assume $\mu \neq 0$ and $\varrho^{\mathsf{T}} b \neq 0$.*

- i) *If $I - M_{\mathcal{S}}$ is nonsingular, then the unique fixed point of $f^{\mathcal{S}}$, $x^{*\mathcal{S}}$, given by (21), lies on the switching manifold if and only if $P_{\mathcal{S}}$ is singular.*
- ii) *If $P_{\mathcal{S}}$ is nonsingular, then $f^{\mathcal{S}}$ has a fixed point if and only if $I - M_{\mathcal{S}}$ is nonsingular.*

Proof. Part (i) follows immediately from (24). If $I - M_{\mathcal{S}}$ is nonsingular, part (ii) is trivial by (21). Suppose $I - M_{\mathcal{S}}$ is singular and suppose for a contradiction $f^{\mathcal{S}}$ has a fixed point $x^{*\mathcal{S}}$. Then by (17) we have

$$(I - M_{\mathcal{S}})x^{*\mathcal{S}} = P_{\mathcal{S}}b\mu .$$

Multiplication of this by $\varrho_{\mathcal{S}}^{\mathsf{T}}$ (22) on the left yields

$$\det(I - M_{\mathcal{S}})s^{*\mathcal{S}} = \det(P_{\mathcal{S}})\varrho^{\mathsf{T}}b\mu ,$$

where we have also used (9) and Lemma 5. This provides a contradiction because the left hand side of the previous equation is zero, whereas by assumption the right hand side is nonzero. \square

5 Generalized shrinking points

At this stage we find it useful to impose the extra assumption that the map (6) under investigation here is piecewise- C^K , for some $K \in \mathbb{N}$. This allows us to derive series expansions of smooth components of the map and iterates of the map. In particular this assumption allows us to apply the center manifold theorem necessary for proving the existence of saddle-node bifurcations in §6.

In order to unfold a generalized shrinking point, we must first give a precise definition of such a point. We use the results of the previous section to write down assumptions that guarantee the existence of a periodic solution with two points on the switching manifold. As in [10], it is useful to assume that this periodic solution is admissible. To state this assumption we need to renormalize the map (6).

Recall that the map (7) depends upon an arbitrary vector of parameters ξ , and that μ denotes the first component of this vector. Scaling x by μ gives a new map h defined through

$$f^J(\mu z; \xi) = \mu h^J(z; \xi) ,$$

where $z \in \mathbb{R}^N$. Note that when f^J is C^K then h^J is C^{K-1} , and using (7), it has the expansion

$$h^J(z; \xi) = b(\xi) + A_J(\xi)z + O(\mu) .$$

For $\mu \geq 0$, the *renormalized* map for z is then

$$z_{n+1} = h(z_n; \xi) = \begin{cases} h^L(z_n; \xi), & u_n \leq 0 \\ h^R(z_n; \xi), & u_n \geq 0 \end{cases} , \quad (25)$$

where

$$u = e_1^\top z .$$

Whenever $\mu \geq 0$, if $x = \mu z$ then $f(x; \xi) = \mu h(z; \xi)$. For any \mathcal{S} -cycle (21), we can also let $x^{*\mathcal{S}}(\xi) = \mu z^{*\mathcal{S}}(\xi)$ so that $z^{*\mathcal{S}}(\xi)$ is C^{K-1} and is a fixed point of $h^\mathcal{S} = h^{\mathcal{S}_{n-1}} \circ \dots \circ h^{\mathcal{S}_0}$. Since (25) is a “blow-up” of phase space, points $z \in \mathbb{R}^N$ are not necessarily near the origin when μ is small. The renormalization effectively transfers the μ -dependence of the piecewise-smooth map from the constant term to the nonlinear terms and this scaling is often helpful in the analysis. Note that (25) has nontrivial dynamics for $\mu = 0$; indeed in this case it is piecewise-linear and identical to the map studied in [10].

We now use Lemma 6 to guarantee the existence of a periodic solution with two points on the switching manifold in terms of singularity of matrices, $P_{\mathcal{S}(i)}$ (19).

Definition 3 (Generalized Shrinking Point). Consider the map (6) with $N \geq 2$ and suppose $\varrho^\top(0)b(0) \neq 0$. Let $\mathcal{S} = \mathcal{S}[\frac{m}{n}, \frac{l}{n}]$ be a rotational symbol sequence with $2 \leq l \leq n-2$. Suppose

$$P_{\mathcal{S}}(0) \text{ and } P_{\mathcal{S}((l-1)d)}(0) \text{ are singular} \quad (\text{the singularity condition}).$$

Let

$$\check{\mathcal{S}} = \mathcal{S}^{\bar{0}} , \quad (26)$$

$$\hat{\mathcal{S}} = \mathcal{S}^{\bar{l}d} , \quad (27)$$

and assume $I - M_{\check{\mathcal{S}}}(0)$ and $I - M_{\hat{\mathcal{S}}}(0)$ are nonsingular. Let $\{\check{x}_i(\xi)\}$ be the unique $\check{\mathcal{S}}$ -cycle near the origin ($\check{x}_0(\xi)$ is given by (21)). Let

$$y_i = \check{z}_i(0) , \quad (28)$$

where $\mu \check{z}_i(\xi) = \check{x}_i(\xi)$. If the orbit $\{y_i\}$ is admissible then we say that (6) is at a *generalized shrinking point* when $\xi = 0$.

The sequences $\check{\mathcal{S}}$ (26) and $\hat{\mathcal{S}}$ (27) are rotational with one less and one more L than $\mathcal{S} = \mathcal{S}[\frac{m}{n}, \frac{l}{n}]$, respectively (specifically, $\check{\mathcal{S}} = \mathcal{S}[\frac{m}{n}, \frac{l-1}{n}]^{(-d)}$ and $\hat{\mathcal{S}} = \mathcal{S}[\frac{m}{n}, \frac{l+1}{n}]$). The periodic solution $\{y_i\}$ is fundamental to the shrinking point. As stated in the following lemma, it has two points on the switching manifold. Moreover if $\{\hat{x}_i(\xi)\}$ denotes the unique $\hat{\mathcal{S}}$ -cycle near the origin, then $\hat{z}_i(0) = \check{z}_i(0) = y_i$. We let

$$t_i = e_1^\top y_i . \quad (29)$$

Lemma 7. *Suppose (6) is at a generalized shrinking point when $\xi = 0$. Then,*

- i) $t_0 = t_{ld} = 0$;*
- ii) $t_d, t_{(l-1)d} < 0, t_{-d}, t_{(l+1)d} > 0$;*
- iii) $\{y_i\}$ has minimal period n ;*

See [10] for a proof. Lemma 7 essentially states that the orbit $\{y_i\}$ appears as in Fig. 8.

A consequence of Lemma 7 is that several important matrices are singular. To see this, first note that the point y_0 is a fixed point of $h^S(y; 0)$. By Lemma 2 and Lemma 7(i), y_0 is also a fixed point of $h^{\mathcal{S}^{\overline{0ld}}}(y; 0)$. Using (12), $\mathcal{S}^{\overline{0ld}} = \mathcal{S}^{(-d)}$, and so y_d is a fixed point of $h^S(y; 0)$. The points y_0 and y_d are distinct (by Lemma 7(iii) and since $\{y_i\}$ is admissible), in other words there are multiple \mathcal{S} -cycles. Hence the matrix $I - M_S(0)$ must be singular and consequently each $P_{\mathcal{S}^{(i)}}(0)$ is singular by Lemma 6(ii) producing the following result (given also in [10]):

Corollary 8. *Suppose (6) is at a generalized shrinking point when $\xi = 0$. Then,*

- i) $I - M_S(0)$ is singular;*
- ii) $P_{\mathcal{S}^{(i)}}(0)$ is singular, for all i .*

For reader convenience let us briefly summarize symbols used:

$$\begin{aligned} x &\in \mathbb{R}^N, & s &= e_1^T x, \\ y_i &= \tilde{z}_i(0) = \hat{z}_i(0), & t &= e_1^T y, \\ \mu z &= x, & u &= e_1^T z. \end{aligned}$$

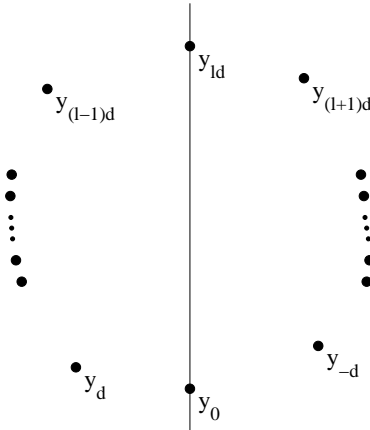


Figure 8: The orbit $\{y_i\}$ as described by Lemma 7. The points y_0 and y_{ld} lie on the switching manifold, $s = 0$.

6 Unfolding generalized shrinking points

We begin by performing a change of coordinates, similar to that in [10], such that, locally, two boundaries of the associated resonance tongue lie on coordinate planes. We are given that $\check{u}_0(\xi)$ and $\check{u}_{ld}(\xi)$ are C^{K-1} and $\check{u}_0(0) = \check{u}_{ld}(0) = 0$ (Lemma 7(i)). Since a generalized shrinking point is a codimension-three phenomenon, we assume there are three bifurcation parameters

$$\xi = (\mu, \eta, \nu) .$$

As long as the matrix

$$\left[\begin{array}{cc} \frac{\partial \check{u}_0}{\partial \eta} & \frac{\partial \check{u}_0}{\partial \nu} \\ \frac{\partial \check{u}_{ld}}{\partial \eta} & \frac{\partial \check{u}_{ld}}{\partial \nu} \end{array} \right] \bigg|_{\xi=0} ,$$

is nonsingular, we may perform a nonlinear coordinate change such that

$$\check{u}_0(\xi) = \eta(1 + O(1)) , \quad (30)$$

$$\check{u}_{ld}(\xi) = \nu(1 + O(1)) . \quad (31)$$

Consequently, on the coordinate plane $\eta = 0$, the point \check{x}_0 of the $\check{\mathcal{S}}$ -cycle lies on the switching manifold. According to Lemma 2, the $\check{\mathcal{S}}$ -cycle is also an $\check{\mathcal{S}}^{\bar{0}} = \mathcal{S}$ -cycle here. Similarly on $\nu = 0$, \check{x}_{ld} lies on the switching manifold. By Lemma 2, here the $\check{\mathcal{S}}$ -cycle is also an $\check{\mathcal{S}}^{\bar{ld}} = \mathcal{S}^{(-d)}$ -cycle (this equality follows simply from (12)). Along the μ -axis (in three-dimensional parameter space) both \check{x}_0 and \check{x}_{ld} lie on the switching manifold so here the $\check{\mathcal{S}}$ -cycle is also an $\hat{\mathcal{S}}$ -cycle. Hence on the μ -axis the orbits $\{\check{x}_i(\xi)\}$ and $\{\hat{x}_i(\xi)\}$ are identical.

In order for ξ to properly unfold a generalized shrinking point we need a nondegeneracy condition on the nonlinear terms of (6) that guarantees the shrinking point breaks apart in the usual manner as μ increases from 0. Along the μ -axis, \check{x}_0 is a fixed point of $f^{\mathcal{S}}$ and when $\mu = 0$ it has an associated multiplier of 1. We will assume that the algebraic multiplicity of this multiplier is one. An appropriate condition on the nonlinear terms is that this multiplier varies linearly (to lowest order) with respect to μ , for small μ . That is, we require

$$\frac{\partial}{\partial \mu} \det (I - D_x f^{\mathcal{S}}(\check{x}_0(\xi); \xi)) \big|_{\xi=0} \neq 0 . \quad (32)$$

We are free to scale the parameter μ before performing the analysis. However, we find it is most instructive to merely fix the sign of μ in a way that ensures resonance arises for $\mu > 0$. It turns out that the following assumption achieves this effect:

$$\text{sgn} \left(\frac{\partial}{\partial \mu} \det (I - D_x f^{\mathcal{S}}(\check{x}_0(\xi); \xi)) \big|_{\xi=0} \right) = \text{sgn}(\det(I - M_{\check{\mathcal{S}}}(0))) . \quad (33)$$

Our unfolding theorem details the existence of admissible periodic solutions in regions of three-dimensional parameter space that are bounded by six different surfaces. As a consequence of the choice (30) and (31), three of these surfaces are simply the coordinate planes. The following lemma gives series expansions of the remaining three surfaces.

Lemma 9. *Suppose the piecewise- C^K map (6) is at a generalized shrinking point when $\xi = 0$ and that $K \geq 4$. Assume that the only eigenvalue of $M_{\mathcal{S}}(0)$ on the unit circle is 1 and that it has algebraic multiplicity one, and that (30), (31) and (33) hold. Let*

$$\check{\delta} = \det(I - M_{\mathcal{S}}(0)) , \quad (34)$$

$$\hat{\delta} = \det(I - M_{\mathcal{S}}(0)) , \quad (35)$$

$$k_0 = \frac{\partial}{\partial \mu} \det(I - D_x f^{\mathcal{S}}(\check{x}_0(\xi); \xi)) \Big|_{\xi=0} , \quad (36)$$

(which are all nonzero due to assumptions in the definition of a generalized shrinking point). Then,

$$i) \quad \frac{\check{\delta}}{\hat{\delta}} = -\frac{t_d t_{(l-1)d}}{t_{-d} t_{(l+1)d}} ;$$

$$ii) \quad \hat{u}_{ld}(\xi) = 0 \text{ on a } C^{K-1} \text{ surface, } \eta = \phi_1(\mu, \nu) = \nu \left(-\frac{k_0 t_d}{\check{\delta} t_{(l+1)d}} \mu - \frac{t_d}{t_{(l-1)d} t_{(l+1)d}} \nu + O(2) \right) ;$$

$$iii) \quad \hat{u}_0(\xi) = 0 \text{ on a } C^{K-1} \text{ surface, } \nu = \phi_2(\mu, \eta) = \eta \left(\frac{k_0 t_{(l-1)d}}{\check{\delta} t_{-d}} \mu - \frac{t_{(l-1)d}}{t_d t_{-d}} \eta + O(2) \right) ;$$

iv) there is a C^{K-2} function given by

$$\Lambda(\xi) = \left(\frac{k_0}{\check{\delta}} \mu + \frac{1}{t_d} \eta + \frac{1}{t_{(l-1)d}} \nu \right)^2 - \frac{4k_0}{\check{\delta} t_d} \mu \eta + o(2) , \quad (37)$$

such that for $\mu > 0$ classical saddle-node bifurcations of \mathcal{S} -cycles occur when $\Lambda(\xi) = 0$ (though are not necessarily admissible);

v) if $\mu > 0$, then $\Lambda(\xi) \leq 0$ only if $\eta \leq 0$ and $\nu \geq \phi_2(\mu, \eta)$; moreover $\Lambda(\xi) = 0$ along $(\mu, 0, \zeta_1(\mu))$ and $(\mu, \zeta_2(\mu), \phi_2(\mu, \zeta_2(\mu)))$ for C^{K-1} functions ζ_1 and ζ_2 ,

$$\zeta_1(\mu) = -\frac{k_0 t_{(l-1)d}}{\check{\delta}} \mu + O(\mu^2) , \quad (38)$$

$$\zeta_2(\mu) = \frac{k_0 t_d}{\check{\delta}} \mu + O(\mu^2) . \quad (39)$$

See Appendix A for a proof. It is useful to consider the nonsingular, linear coordinate change:

$$\begin{bmatrix} \tilde{\mu} \\ \tilde{\eta} \\ \tilde{\nu} \end{bmatrix} = \begin{bmatrix} \frac{k_0}{\check{\delta}} & -\frac{1}{t_d} & \frac{1}{t_{(l-1)d}} \\ 0 & -\frac{1}{t_d} & -\frac{1}{t_{(l-1)d}} \\ 0 & \frac{1}{t_d} & -\frac{1}{t_{(l-1)d}} \end{bmatrix} \begin{bmatrix} \mu \\ \eta \\ \nu \end{bmatrix} , \quad (40)$$

because substitution of (40) into (37) produces

$$\Lambda(\xi) = \tilde{\mu}^2 + \tilde{\eta}^2 - \tilde{\nu}^2 + o(2) . \quad (41)$$

In this alternative coordinate system, saddle-node bifurcations occur approximately on a cone. All six surfaces are sketched for $\mu \geq 0$ in Fig. 9. The surface $\Lambda(\xi) = 0$ intersects the plane $\eta = 0$ tangentially along the curve $(\mu, 0, \zeta_1(\mu))$ and the surface $\nu = \phi_2(\mu, \eta)$ tangentially along the curve $(\mu, \zeta_2(\mu), \phi_2(\mu, \zeta_2(\mu)))$.

Different two-dimensional slices of parameter space through Fig. 9 will produce vastly different bifurcation sets. Since slices defined by fixing the value of μ have been shown earlier (see Fig. 6), in Fig. 9 we draw a plane at fixed $\mu > 0$ and show its curves of intersection with the nearby surfaces. This cross-section is shown again in Fig. 10. A close inspection of the formulas for ϕ_1 and ϕ_2 given Lemma 9 reveal a specific geometrical arrangement near the generalized shrinking point as follows. Since $t_d < 0$, $t_{(l+1)d} > 0$ (Lemma 7(ii)) and $\text{sgn}(k_0) = \text{sgn}(\delta)$ (33), the coefficient for the $\mu\nu$ term of $\phi_1(\mu, \nu)$ is positive. Consequently, for small $\mu > 0$ the angle θ_2 in Fig. 10 is greater than 90° . Similarly the coefficient for the $\mu\eta$ term of $\phi_2(\mu, \eta)$ is negative and so $\theta_1 < 90^\circ$. Any smooth distortion of Fig. 10 will preserve the property $\theta_1 < \theta_2$. The curves $\eta = \phi_1(\mu, \nu)$ and $\nu = \phi_2(\mu, \eta)$ bend left and down because the ν^2 term of $\phi_1(\mu, \nu)$ and the η^2 term of $\phi_2(\mu, \eta)$ are both negative. The saddle-node locus is approximately a parabola.

Finally, we present the main result. See Appendix A for a proof.

Theorem 10. *Suppose (6) is at a generalized shrinking point when $\xi = 0$ and that $K \geq 4$. Assume that the only eigenvalue of $M_S(0)$ on the unit circle is 1 and that it has algebraic multiplicity one. Assume y_0 and y_{ld} are the only points of $\{y_i\}$ that lie on the switching manifold. Assume we have (30), (31) and (33). Let*

$$\begin{aligned} \Psi_1 &= \{ \xi \in \mathbb{R}^3 \mid \mu > 0, \eta > 0, \nu > 0 \} , \\ \Psi_2 &= \{ \xi \in \mathbb{R}^3 \mid \mu > 0, \eta < \phi_1(\mu, \nu), \nu < \phi_2(\mu, \eta) \} , \\ \Psi_3 &= \{ \xi \in \mathbb{R}^3 \mid \mu > 0, \zeta_2(\mu) < \eta < 0, \phi_2(\mu, \eta) < \nu < \zeta_1(\mu), \Lambda(\xi) > 0 \} , \end{aligned}$$

for the functions described in Lemma 9 (see Fig. 10).

Then, in Ψ_1 , \mathcal{S} and $\tilde{\mathcal{S}}$ -cycles are admissible and collide in border-collision fold bifurcations on $\nu = 0$ and $\eta = 0$ for $\nu > \zeta_1(\mu)$, in Ψ_2 , \mathcal{S} and $\tilde{\mathcal{S}}$ -cycles are admissible and collide in border-collision fold bifurcations on $\eta = \phi_1(\mu, \nu)$ and $\nu = \phi_2(\mu, \eta)$ for $\eta < \zeta_2(\mu)$, in Ψ_3 , two \mathcal{S} -cycles are admissible and collide in classical saddle-node bifurcations where $\Lambda(\xi) = 0$; the boundaries $\eta = 0$ and $\nu = \phi_2(\mu, \eta)$ correspond to border-collision persistence.

7 Conclusions

We have studied resonance arising from an arbitrary border-collision bifurcation of a piecewise-smooth, continuous map. When a periodic solution created in a border-collision bifurcation is rotational, in the sense described in §3, the corresponding resonance tongue typically has a sausage-like geometry, see Fig. 3. Shrinking points break apart as parameters are varied

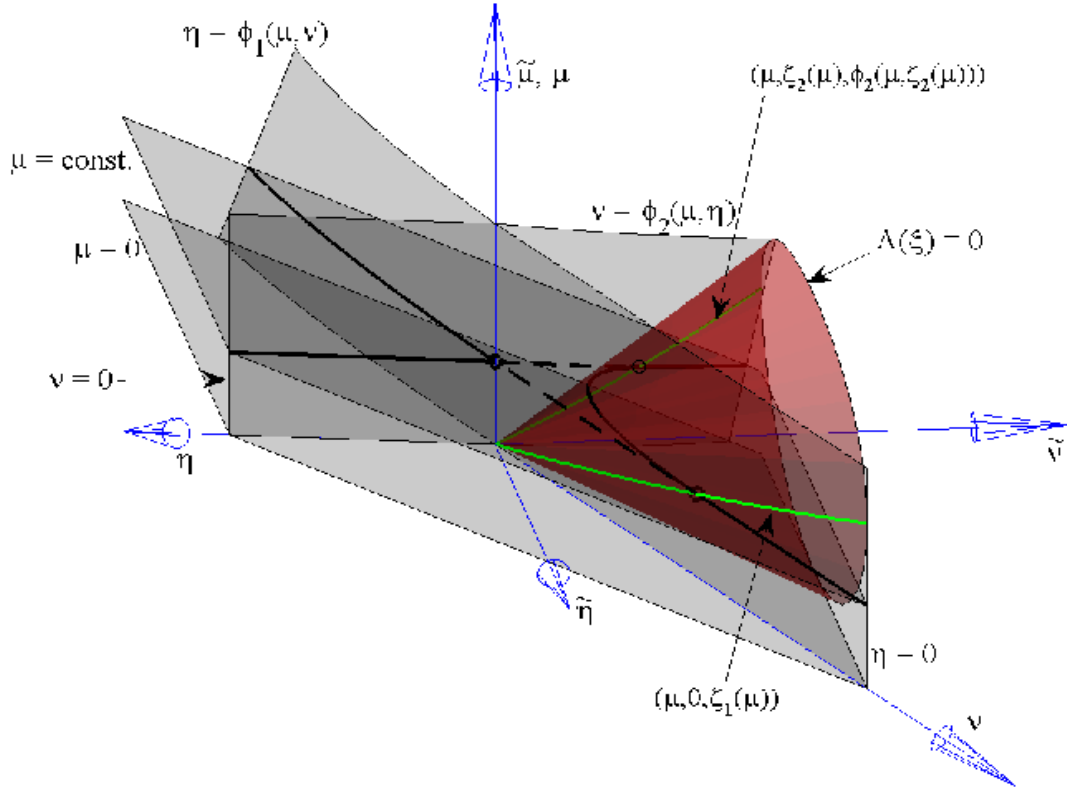


Figure 9: The three-dimensional unfolding of a generalized shrinking point for the piecewise-smooth, continuous map (6). The surface $\mu = 0$ corresponds to the border-collision bifurcation of a fixed point. On each of the four surfaces, $\eta = 0$, $\nu = 0$, $\eta = \phi_1(\mu, \nu)$ and $\nu = \phi_2(\mu, \eta)$ (which share a mutual intersection with the μ -axis), one point of an \mathcal{S} -cycle lies on the switching manifold. The surface $\Lambda(\xi) = 0$ corresponds to classical saddle-node bifurcations of an \mathcal{S} -cycle. This surface is approximately a cone, as made evident by transformation to the alternative $(\tilde{\mu}, \tilde{\eta}, \tilde{\nu})$ -coordinate system, (40), and tangentially intersects $\eta = 0$ and $\nu = \phi_2(\mu, \eta)$ along the curves $(\mu, 0, \zeta_1(\mu))$ and $(\mu, \zeta_2(\mu), \phi_2(\mu, \zeta_2(\mu)))$, respectively. The plane $\mu = \text{const.}$ illustrates the cross-section shown in Fig. 10.

to move away from the border-collision bifurcation, Fig. 6. We have proved Thm. 10 which details the manner by which shrinking point destruction occurs. The results of the theorem are in complete agreement with numerical results, Figs. 5 and 6. Theorem 10 does not provide an understanding of global properties of resonance tongues, for instance the observation that the majority of, or perhaps all of, the kinks in the resonance tongues of Fig. 5 appear on the left sides of the tongues.

If the map (6) has an invariant circle that intersects the switching manifold at two points

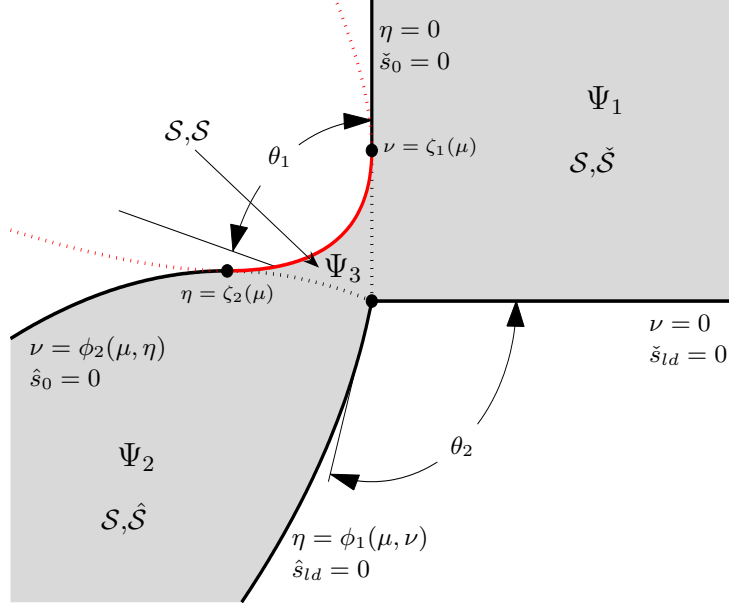


Figure 10: A two-parameter bifurcation diagram for the map (6) near a generalized shrinking point for fixed, small $\mu > 0$. As stated in Thm. 10, an admissible \mathcal{S} -cycle coexists with, (i) an admissible $\tilde{\mathcal{S}}$ -cycle in Ψ_1 ; (ii) an admissible $\hat{\mathcal{S}}$ -cycle in Ψ_2 ; (iii) a second admissible \mathcal{S} -cycle in Ψ_3 . Along the solid curves the two coexisting, admissible, periodic solutions undergo a border-collision fold bifurcation except on the curve connecting the points $\nu = \zeta_1(\mu)$ and $\eta = \zeta_2(\mu)$ which corresponds to a classical saddle-node bifurcation of the two periodic solutions. The boundary between Ψ_1 and Ψ_3 and the boundary between Ψ_2 and Ψ_3 correspond to border-collision persistence.

and the restriction of the map to the circle is a homeomorphism, then any periodic solution on the circle will have a corresponding symbol sequence that is rotational. Our results do not apply to periodic solutions born in border-collision bifurcations that are non-rotational. However such periodic solutions seem to be, in some sense, less common [12]. Note that we make no requirement that (6) is a homeomorphism or has an invariant circle, only that corresponding periodic solutions are rotational.

A limitation of Thm. 10 is that it includes the assumption that the map (6) is piecewise- C^K . Poincaré maps relating to sliding phenomena are generically piecewise-smooth, continuous with a $\frac{3}{2}, 2, \frac{5}{2}, \dots$ type power expansion [5] and hence not apply to Thm. 10. It seems reasonable that in this case a similar result with different scaling laws could apply. A major hurdle in the analysis is that the center manifold theorem (applied in the proof of Thm. 10) is not immediately applicable to non-integer power expansions.

In our definition of the codimension-three generalized shrinking point (Def. 3), we require that both matrices $I - M_{\tilde{\mathcal{S}}}$ and $I - M_{\hat{\mathcal{S}}}$ are nonsingular at $\xi = 0$. We then prove Lemma 9 by computing parameter-dependent series expansions (see Appendix A). However part (i) of Lemma 9 is independent of the parameters and it seems there should be a more direct proof of this result. This problem remains for future work. Related problems that remain to be fully understood include the persistence of invariant topological circles created at border-

collision bifurcations and the simultaneous occurrence of a border-collision bifurcation with a classical Neimark-Sacker bifurcation.

A Proofs for Section 6

Proof of Lemma 9. We divide the proof into four major steps. In the first step we use the formulas for $\tilde{u}_0(\xi)$ (30) and $\tilde{u}_{ld}(\xi)$ (31) to derive formulas for \hat{u}_0 and \hat{u}_{ld} , enabling us to compute the border-collision boundaries $\eta = \phi_1(\mu, \nu)$ and $\nu = \phi_2(\mu, \eta)$. The method used is an extension of Lemma 3 of [10] to account for the nonlinear terms in (6). In step 2 we continue this methodology to derive identities relating coefficients, verify (i) of the lemma and refine the formulas for ϕ_1 and ϕ_2 . In the third step we compute the one-dimensional center manifold of f^S to identify saddle-node bifurcations on the surface $\Lambda = 0$. Lastly, in step 4 we study at the intersections of $\Lambda = 0$ with $\eta = 0$ and $\nu = \phi_2(\mu, \eta)$ to complete the proof. For convenience we write

$$\det(I - M_S(0, \eta, \nu)) = k_1\eta + k_2\nu + O(2) . \quad (42)$$

Step 1: *Derive formulas for \hat{u}_0 and \hat{u}_{ld} and define ϕ_1 and ϕ_2 .*

Periodic solutions of (6) with associated symbol sequences that differ by a single symbol may be related algebraically (as shown below). However the sequences \check{S} and \hat{S} differ in two symbols, so in general we cannot effectively compare the \check{S} and \hat{S} -cycles. But if one of the four important quantities, \tilde{u}_0 , \tilde{u}_{ld} , \hat{u}_0 and \hat{u}_{ld} is zero, then one of the two n -cycles is also an S -cycle and the two n -cycles may indeed be effectively related. The four curves which make up the edges of a resonance tongue near a shrinking point correspond to where these four quantities are zero. We separate this step of the proof by where different assumptions on the parameters are made.

a) *Suppose $\eta = 0$.* Then by (30), $\tilde{u}_0 = 0$. Thus the \check{S} -cycle, $\{\tilde{x}_i\}$, is also an S -cycle. So each \tilde{x}_i is a fixed point of $f^{S^{(i)}}$. In particular, \tilde{x}_{ld} is a fixed point of $f^{S^{(ld)}}$, which in the renormalized frame (25) says that \tilde{z}_{ld} is a fixed point of $h^{S^{(ld)}}$:

$$\tilde{z}_{ld}(\mu, 0, \nu) = h^{S^{(ld)}}(\tilde{z}_{ld}(\mu, 0, \nu); \mu, 0, \nu) .$$

Expressing $h^{S^{(ld)}}$ as a Taylor series centered at y_{ld} (28) and evaluated at \tilde{z}_{ld} yields

$$\tilde{z}_{ld}(\mu, 0, \nu) = h^{S^{(ld)}}(y_{ld}; \mu, 0, \nu) + D_z h^{S^{(ld)}}(y_{ld}; \mu, 0, \nu)(\tilde{z}_{ld}(\mu, 0, \nu) - y_{ld}) + O(3) , \quad (43)$$

where the next term in the expansion is $O(\mu)O(|\tilde{z}_{ld}(\mu, 0, \nu) - y_{ld}|^2)$ which is $O(3)$ because $\tilde{z}_{ld}(0, 0, 0) = y_{ld}$.

Now, \hat{z}_{ld} is a fixed point of $h^{\hat{S}^{(ld)}}$ (for any sufficiently small ξ), therefore

$$\hat{z}_{ld}(\mu, 0, \nu) = h^{\hat{S}^{(ld)}}(y_{ld}; \mu, 0, \nu) + D_z h^{\hat{S}^{(ld)}}(y_{ld}; \mu, 0, \nu)(\hat{z}_{ld}(\mu, 0, \nu) - y_{ld}) + O(3) , \quad (44)$$

where the right-hand side is the Taylor series of $h^{\hat{S}^{(ld)}}$ centered at y_{ld} . But $S^{(ld)} = \hat{S}^{(ld)\bar{0}}$ (refer to §3), thus whenever $u = e_1^T z = 0$, we have $h^{S^{(ld)}}(z; \xi) = h^{\hat{S}^{(ld)}}(z; \xi)$ (by continuity of (6)). Since $t_{ld} = e_1^T y_{ld} = 0$ (Lemma 7(i)), we have

$$h^{S^{(ld)}}(y_{ld}; \mu, 0, \nu) = h^{\hat{S}^{(ld)}}(y_{ld}; \mu, 0, \nu) . \quad (45)$$

Furthermore, although in general the last $N-1$ columns of $D_z h^{\mathcal{S}^{(ld)}}$ and $D_z h^{\hat{\mathcal{S}}^{(ld)}}$ are not equal, since $h^{\mathcal{S}^{(ld)}} \equiv h^{\hat{\mathcal{S}}^{(ld)}}$ on the switching manifold, the last $N-1$ columns of $D_z h^{\mathcal{S}^{(ld)}}(y_{ld}; \mu, 0, \nu)$ and $D_z h^{\hat{\mathcal{S}}^{(ld)}}(y_{ld}; \mu, 0, \nu)$ are indeed equal. Consequently the first row of their adjugates is the same:

$$e_1^\top \text{adj}(I - D_z h^{\mathcal{S}^{(ld)}}(y_{ld}; \mu, 0, \nu)) = e_1^\top \text{adj}(I - D_z h^{\hat{\mathcal{S}}^{(ld)}}(y_{ld}; \mu, 0, \nu)) . \quad (46)$$

The combination of (43), (44), (45) and $t_{ld} = 0$ produces

$$(I - D_z h^{\mathcal{S}^{(ld)}}(y_{ld}; \mu, 0, \nu)) \tilde{z}_{ld}(\mu, 0, \nu) = (I - D_z h^{\hat{\mathcal{S}}^{(ld)}}(y_{ld}; \mu, 0, \nu)) \hat{z}_{ld}(\mu, 0, \nu) + O(3) , \quad (47)$$

and multiplication of both sides of (47) by (46) on the left (remembering (9) and $u_i = e_1^\top z_i$) leads to

$$\det(I - D_z h^{\mathcal{S}^{(ld)}}(y_{ld}; \mu, 0, \nu)) \tilde{u}_{ld}(\mu, 0, \nu) = \det(I - D_z h^{\hat{\mathcal{S}}^{(ld)}}(y_{ld}; \mu, 0, \nu)) \hat{u}_{ld}(\mu, 0, \nu) + O(3) .$$

We now plug in known expansions (\tilde{u}_{ld} is given by (31), $\det(I - D_z h^{\hat{\mathcal{S}}^{(ld)}}(y_{ld}; \mu, 0, \nu)) = \hat{\delta} + O(1)$ by (35) and Lemma 3, $\det(I - D_z h^{\mathcal{S}^{(ld)}}(y_{ld}; \mu, 0, \nu)) = k_0\mu + k_2\nu + O(2)$ by (36), (42) and Lemma 3):

$$(k_0\mu + k_2\nu + O(2))\nu(1 + O(1)) = (\hat{\delta} + O(1))\hat{u}_{ld}(\mu, 0, \nu) ,$$

which, upon rearranging, produces the following useful expression:

$$\hat{u}_{ld}(\mu, 0, \nu) = \frac{k_0}{\hat{\delta}}\mu\nu + \frac{k_2}{\hat{\delta}}\nu^2 + O(3) . \quad (48)$$

Below we use the same approach to derive further expressions for \hat{u}_0 and \hat{u}_{ld} with different assumptions on the parameters. For brevity we will not provide the same level of detail.

b) Suppose $\eta = 0$ and $\mu = 0$. As above, since $\eta = 0$, the $\tilde{\mathcal{S}}$ -cycle is also an \mathcal{S} -cycle. In particular, \tilde{z}_{-d} is a fixed point of $h^{\mathcal{S}^{(-d)}}$. Here we express $h^{\mathcal{S}^{(-d)}}$ as a Taylor series centered at y_0 (the reason for choosing y_0 will soon become clear) and evaluated at \tilde{z}_{-d} :

$$\tilde{z}_{-d}(0, 0, \nu) = h^{\mathcal{S}^{(-d)}}(y_0; 0, 0, \nu) + D_z h^{\mathcal{S}^{(-d)}}(y_0; 0, 0, \nu)(\tilde{z}_{-d}(0, 0, \nu) - y_0) , \quad (49)$$

where, unlike in (43), there is no next term in the expansion when $\mu = 0$ the map is affine. Now, \hat{z}_0 is a fixed point of $h^{\hat{\mathcal{S}}}$, therefore

$$\hat{z}_0(0, 0, \nu) = h^{\hat{\mathcal{S}}}(y_0; 0, 0, \nu) + D_z h^{\hat{\mathcal{S}}}(y_0; 0, 0, \nu)(\hat{z}_0(0, 0, \nu) - y_0) . \quad (50)$$

But $\mathcal{S}^{(-d)} = \hat{\mathcal{S}}^{\bar{0}}$ (by (12)), and since $t_0 = 0$ (Lemma 7(i)) we may perform the same simplification that we did above to combine (49) and (50) leaving

$$\begin{aligned} (I - D_z h^{\mathcal{S}^{(-d)}}(y_0; 0, 0, \nu)) \tilde{z}_{-d}(0, 0, \nu) &= (I - D_z h^{\hat{\mathcal{S}}}(y_0; 0, 0, \nu)) \hat{z}_0(0, 0, \nu) , \\ \Rightarrow \det(I - D_z h^{\mathcal{S}^{(-d)}}(y_0; 0, 0, \nu)) \tilde{u}_{-d}(0, 0, \nu) &= \det(I - D_z h^{\hat{\mathcal{S}}}(y_0; 0, 0, \nu)) \hat{u}_0(0, 0, \nu) , \\ \Rightarrow (k_2\nu + O(\nu^2))(t_{-d} + O(\nu)) &= (\hat{\delta} + O(\nu))\hat{u}_0(0, 0, \nu) , \\ \Rightarrow \hat{u}_0(0, 0, \nu) &= \frac{k_2 t_{-d}}{\hat{\delta}}\nu + O(\nu^2) . \end{aligned} \quad (51)$$

c) Suppose $\nu = 0$. As discussed in §6, when $\nu = 0$ the $\check{\mathcal{S}}$ -cycle is also an $\mathcal{S}^{(-d)}$ -cycle. Therefore \check{z}_0 is a fixed point of $h^{\mathcal{S}^{(-d)}}$ and so

$$\check{z}_0(\mu, \eta, 0) = h^{\mathcal{S}^{(-d)}}(y_0; \mu, \eta, 0) + D_z h^{\mathcal{S}^{(-d)}}(y_0; \mu, \eta, 0)(\check{z}_0(\mu, \eta, 0) - y_0) + O(3). \quad (52)$$

Also, \hat{z}_0 is a fixed point of $h^{\hat{\mathcal{S}}}$, thus

$$\hat{z}_0(\mu, \eta, 0) = h^{\hat{\mathcal{S}}}(y_0; \mu, \eta, 0) + D_z h^{\hat{\mathcal{S}}}(y_0; \mu, \eta, 0)(\hat{z}_0(\mu, \eta, 0) - y_0) + O(3). \quad (53)$$

Combining (52) and (53) leads to (since $\mathcal{S}^{(-d)} = \hat{\mathcal{S}}^{\bar{0}}$)

$$\det(I - D_z h^{\mathcal{S}^{(-d)}}(y_0; \mu, \eta, 0))\check{u}_0(\mu, \eta, 0) = \det(I - D_z h^{\hat{\mathcal{S}}}(y_0; \mu, \eta, 0))\hat{u}_0(\mu, \eta, 0) + O(3).$$

Take care to note that

$$\tilde{k}_0 \equiv \frac{\partial}{\partial \mu} \det(I - D_x f^{\mathcal{S}}(\check{x}_d(\xi); \xi)) \Big|_{\xi=0}, \quad (54)$$

is different to (32) due to the presence of nonlinear terms in (6) (below we will show that in fact $\tilde{k}_0 = -k_0$). Consequently

$$\begin{aligned} (\tilde{k}_0 \mu + k_1 \eta + O(2))\eta(1 + O(1)) &= (\hat{\delta} + O(1))\hat{u}_0(\mu, \eta, 0), \\ \Rightarrow \hat{u}_0(\mu, \eta, 0) &= \frac{\tilde{k}_0}{\hat{\delta}}\mu\eta + \frac{k_1}{\hat{\delta}}\eta^2 + O(3). \end{aligned} \quad (55)$$

d) Suppose $\nu = 0$ and $\mu = 0$. Here $\check{z}_{(l+1)d}$ is a fixed point of $h^{\mathcal{S}^{(ld)}}$, so

$$\check{z}_{(l+1)d}(0, \eta, 0) = h^{\mathcal{S}^{(ld)}}(y_{ld}; 0, \eta, 0) + D_z h^{\mathcal{S}^{(ld)}}(y_{ld}; 0, \eta, 0)(\check{z}_{(l+1)d}(0, \eta, 0) - y_{ld}), \quad (56)$$

and \hat{z}_{ld} is a fixed point of $h^{\hat{\mathcal{S}}^{(ld)}}$, so

$$\hat{z}_{ld}(0, \eta, 0) = h^{\hat{\mathcal{S}}^{(ld)}}(y_{ld}; 0, \eta, 0) + D_z h^{\hat{\mathcal{S}}^{(ld)}}(y_{ld}; 0, \eta, 0)(\hat{z}_{ld}(0, \eta, 0) - y_{ld}), \quad (57)$$

and since $\mathcal{S}^{(ld)} = \hat{\mathcal{S}}^{(ld)\bar{0}}$ we obtain

$$\begin{aligned} \det(I - D_z h^{\mathcal{S}^{(ld)}}(y_{ld}; 0, \eta, 0))\check{u}_{(l+1)d}(0, \eta, 0) &= \det(I - D_z h^{\hat{\mathcal{S}}^{(ld)}}(y_{ld}; 0, \eta, 0))\hat{u}_{ld}(0, \eta, 0), \\ \Rightarrow (k_1 \eta + O(\eta^2))(t_{(l+1)d} + O(\eta)) &= (\hat{\delta} + O(\eta))\hat{u}_{ld}(0, \eta, 0), \\ \Rightarrow \hat{u}_{ld}(0, \eta, 0) &= \frac{k_1 t_{(l+1)d}}{\hat{\delta}}\eta + O(\eta^2). \end{aligned} \quad (58)$$

We now apply the implicit function theorem to the C^{K-1} function $\hat{u}_{ld}(\xi)$. By (48) and (58), there exists a unique C^{K-1} function ϕ_1 such that for small μ and ν , $\hat{u}_{ld}(\mu, \phi_1(\mu, \nu), \nu) = 0$ and

$$\phi_1(\mu, \nu) = -\frac{k_0}{k_1 t_{(l+1)d}}\mu\nu - \frac{k_2}{k_1 t_{(l+1)d}}\nu^2 + O(3). \quad (59)$$

Recall that $\check{u}_{ld} = 0$ along the μ -axis (a consequence of (30) and (31)), therefore $\phi_1 = 0$ whenever $\nu = 0$. Thus we may rewrite (59) as

$$\phi_1(\mu, \nu) = \nu \left(-\frac{k_0}{k_1 t_{(l+1)d}}\mu - \frac{k_2}{k_1 t_{(l+1)d}}\nu + O(2) \right). \quad (60)$$

Similarly by (51) and (55), there exists a unique C^{K-1} function ϕ_2 such that for small μ and η , $\hat{u}_0(\mu, \eta, \phi_2(\mu, \eta)) = 0$ and

$$\phi_2(\mu, \eta) = \eta \left(-\frac{\tilde{k}_0}{k_2 t_{-d}} \mu - \frac{k_1}{k_2 t_{-d}} \eta + O(2) \right), \quad (61)$$

where the η may be factored in the same fashion as for (60).

Step 2: Verify (i) of the lemma and refine the formulas for ϕ_1 and ϕ_2 , (60) and (61).

Here we continue to employ the methodology above to compare the $\tilde{\mathcal{S}}$ and $\hat{\mathcal{S}}$ -cycles.

a) Suppose $\eta = \phi_1(\mu, \nu)$. Then $\hat{u}_{ld} = 0$, and so the $\hat{\mathcal{S}}$ -cycle is also an \mathcal{S} -cycle. Thus, in particular, \hat{z}_0 is a fixed point of $h^{\mathcal{S}}$:

$$\begin{aligned} \hat{z}_0(\mu, \phi_1(\mu, \nu), \nu) &= h^{\mathcal{S}}(y_0; \mu, \phi_1(\mu, \nu), \nu) \\ &\quad + D_z h^{\mathcal{S}}(y_0; \mu, \phi_1(\mu, \nu), \nu) (\hat{z}_0(\mu, \phi_1(\mu, \nu), \nu) - y_0) + O(3). \end{aligned}$$

Also \check{z}_0 is a fixed point of $h^{\tilde{\mathcal{S}}}$:

$$\begin{aligned} \check{z}_0(\mu, \phi_1(\mu, \nu), \nu) &= h^{\tilde{\mathcal{S}}}(y_0; \mu, \phi_1(\mu, \nu), \nu) \\ &\quad + D_z h^{\tilde{\mathcal{S}}}(y_0; \mu, \phi_1(\mu, \nu), \nu) (\check{z}_0(\mu, \phi_1(\mu, \nu), \nu) - y_0) + O(3). \end{aligned}$$

Then, since $\mathcal{S} = \tilde{\mathcal{S}}^{\bar{0}}$,

$$\begin{aligned} \det(I - D_z h^{\mathcal{S}}(y_0; \mu, \phi_1(\mu, \nu), \nu)) \hat{u}_0(\mu, \phi_1(\mu, \nu), \nu) &= \\ \det(I - D_z h^{\tilde{\mathcal{S}}}(y_0; \mu, \phi_1(\mu, \nu), \nu)) \check{u}_0(\mu, \phi_1(\mu, \nu), \nu) &+ O(3). \end{aligned} \quad (62)$$

Unlike for similar expressions in Step 1, we have already determined an expansion for each of the four components of (62) (in particular $\hat{u}_0(\mu, \phi_1(\mu, \nu), \nu)$ is given by (51), (55) and (60) and $\check{u}_0(\mu, \phi_1(\mu, \nu), \nu)$ is given by (30) and (60), also recall Lemma 3):

$$\begin{aligned} (k_0 \mu + k_2 \nu + O(2)) \left(\frac{k_2 t_{-d}}{\delta} \nu + O(2) \right) &= \\ (\check{\delta} + O(1)) \left(-\frac{k_0}{k_1 t_{(l+1)d}} \mu \nu - \frac{k_2}{k_1 t_{(l+1)d}} \nu^2 + O(3) \right) &+ O(3). \end{aligned}$$

Equating the second-order coefficients produces

$$k_1 k_2 t_{(l+1)d} t_{-d} = -\check{\delta} \hat{\delta}. \quad (63)$$

b) Suppose $\eta = \phi_1(\mu, \nu)$ and $\mu = 0$. In the same manner as above, equating the first components of the power series of $h^{\mathcal{S}^{((l-1)d)}}$ and $h^{\tilde{\mathcal{S}}^{(ld)}}$ yields

$$\begin{aligned} \det(I - D_z h^{\mathcal{S}^{((l-1)d)}}(y_{ld}; 0, \phi_1(0, \nu), \nu) \hat{u}_{(l-1)d}(0, \phi_1(0, \nu), \nu) &= \\ \det(I - D_z h^{\tilde{\mathcal{S}}^{(ld)}}(y_{ld}; 0, \phi_1(0, \nu), \nu) \check{u}_{ld}(0, \phi_1(0, \nu), \nu) &, \end{aligned}$$

and since $\mathcal{S}^{((l-1)d)} = \tilde{\mathcal{S}}^{(ld)\bar{0}}$,

$$\begin{aligned} (k_2 \nu + O(\nu^2))(t_{(l-1)d} + O(\nu)) &= (\check{\delta} + O(\nu))(\nu + O(\nu^2)), \\ \Rightarrow k_2 &= \frac{\check{\delta}}{t_{(l-1)d}}. \end{aligned} \quad (64)$$

c) Suppose $\nu = \phi_2(\mu, \eta)$ and $\mu = 0$. Here, equating the first components of h^S and $h^{\tilde{S}}$ produces

$$\begin{aligned} \det(I - D_z h^S(y_0; 0, \eta, \phi_2(0, \eta)) \hat{u}_d(0, \eta, \phi_2(0, \eta)) = \\ \det(I - D_z h^{\tilde{S}}(y_0; 0, \eta, \phi_2(0, \eta)) \check{u}_0(0, \eta, \phi_2(0, \eta)) , \end{aligned}$$

from which it follows that

$$\begin{aligned} (k_1 \eta + O(\eta^2))(t_d + O(\eta)) &= (\check{\delta} + O(\eta))(\eta + O(\eta^2)) , \\ \Rightarrow k_1 &= \frac{\check{\delta}}{t_d} . \end{aligned} \tag{65}$$

We now combine above equations to demonstrate some parts of the lemma. By combining (63), (64) and (65) we obtain (i). Combining (60), (64) and (65) verifies (ii). Combining (61), (64) and (65) will verify (iii) once it is shown that $\tilde{k}_0 = -k_0$ (see below).

Step 3: *Derive and analyze the one-dimensional center manifold of f^S to obtain the function $\Lambda(\xi)$ and identify saddle-node bifurcations of \mathcal{S} -cycles.*

When $\xi \equiv (\mu, \eta, \nu) = 0$, $x = 0$ is a fixed point of $f^S(x; \xi)$ and the associated stability multipliers are the eigenvalues of $D_x f^S(0; 0) = M_S(0)$. The matrix $M_S(0)$ has an eigenvalue 1 of algebraic multiplicity one. Let $v \in \mathbb{R}^N$ be the associated eigenvector, i.e. $M_S(0)v = v$. Notice $v \neq 0$ implies $e_1^\top v \neq 0$ since if not then $M_{\mathcal{S}\bar{0}}(0)v = v$ which contradicts the assumption that $I - M_{\mathcal{S}}(0)$ is nonsingular (Def. 3). In what follows we assume $e_1^\top v = 1$.

We now compute the restriction of f^S to the one-dimensional center manifold. Let

$$F(x; \xi) = \begin{bmatrix} f^S(x; \xi) \\ \xi \end{bmatrix} ,$$

denote the $(N + 3)$ -dimensional, C^K , extended map. The Jacobian,

$$DF(0; 0) = \left[\begin{array}{c|ccc} M_S(0) & P_S(0)b(0) & 0 & 0 \\ \hline 0 & & I & \end{array} \right] , \tag{66}$$

has a four-dimensional centerspace, $E^c \in \mathbb{R}^{N+3}$, spanned by

$$\left\{ \begin{bmatrix} \frac{v}{0} \\ 0 \\ 0 \end{bmatrix} , \begin{bmatrix} \frac{y_0}{1} \\ 0 \\ 0 \end{bmatrix} , \begin{bmatrix} 0 \\ 0 \\ 1 \\ 0 \end{bmatrix} , \begin{bmatrix} 0 \\ 0 \\ 0 \\ 1 \end{bmatrix} \right\} ,$$

since, in particular, $y_0 = h^S(y_0; 0) = M_S(0)y_0 + P_S(0)b(0)$.

Since $e_1^\top v = 1$, we may use the center manifold theorem to express the local center manifold, W^c , of f^S , in terms of $s = e_1^\top x$ and ξ . In particular, on W^c ,

$$x = X(s; \xi) = sv + \mu y_0 + O(2) , \tag{67}$$

where $X : \mathbb{R} \times \mathbb{R}^3 \rightarrow \mathbb{R}^N$ is C^{K-1} . The first component of the restriction of f^S to W^c is given by

$$\begin{aligned} s'(s; \xi) &= e_1^\top f^S(X(s; \xi); \xi) \\ &= e_1^\top \mu P_S(0)b(0) + e_1^\top M_S(0)(sv + \mu y_0) + O(2) \\ &= e_1^\top (P_S(0)b(0) + M_S(0)y_0)\mu + e_1^\top M_S(0)vs + O(2) \\ &= s + O(2), \end{aligned}$$

since $e_1^\top (P_S(0)b(0) + M_S(0)y_0) = e_1^\top y_0 = t_0 = 0$ and $e_1^\top M_S(0)v = e_1^\top v = 1$. However we require the knowledge of second order terms of $s'(s; \xi)$, so write

$$s'(s; \xi) = s + c_1 s^2 + c_2 \mu s + c_3 \eta s + c_4 \nu s + c_5 \mu^2 + c_6 \mu \eta + c_7 \mu \nu + c_8 \eta^2 + c_9 \eta \nu + c_{10} \nu^2 + O(3). \quad (68)$$

We now utilize known properties of f^S to determine an expression for the majority of the coefficients, c_i .

- 1) When $\mu = 0$, $x = 0$ is a fixed point of f^S , thus $s'(0; 0, \eta, \nu) = 0$, hence $c_8 = c_9 = c_{10} = 0$.
- 2) When $\eta = 0$, $x = \tilde{x}_0$ is a fixed point of f^S and since here $s = \tilde{s}_0 = 0$, we have $s'(0; \mu, 0, \nu) = 0$, hence $c_5 = c_7 = 0$.
- 3) Similarly when $\nu = 0$, $x = \tilde{x}_d$ is a fixed point of f^S . Here $s = \tilde{s}_d = \tilde{u}_d \mu = t_d \mu + O(2)$, thus $s'(\tilde{u}_d \mu; \mu, \eta, 0) = \tilde{u}_d \mu$, leading to

$$c_1 = -\frac{c_2}{t_d}, \quad c_6 = -c_3 t_d.$$

Thus we have reduced the center manifold map (68) to

$$s'(s; \xi) = s - \frac{c_2}{t_d} s^2 + c_2 \mu s + c_3 \eta s + c_4 \nu s - c_3 t_d \mu \eta + O(3). \quad (69)$$

- 4) Let $\lambda(\eta, \nu)$ be the eigenvalue of $D_x f^S(0; 0, \eta, \nu)$, C^{K-1} dependent on η and ν , for which $\lambda(0, 0) = 1$. This eigenvalue is also the stability multiplier of the fixed point, $s = 0$, of $s'(s; 0, \eta, \nu)$, that is, by (69)

$$\lambda(\eta, \nu) = \frac{\partial s'}{\partial s}(0; 0, \eta, \nu) = 1 + c_3 \eta + c_4 \nu + O(2). \quad (70)$$

Now, $\det(I - D_x f^S(0; 0, \eta, \nu))$ is equal to the product of all N eigenvalues (counting algebraic multiplicity) of $I - D_x f^S(0; 0, \eta, \nu)$. Thus

$$\det(I - D_x f^S(0; 0, \eta, \nu)) = (1 - \lambda(\eta, \nu)) \mathcal{P}(\eta, \nu),$$

where $\mathcal{P}(\eta, \nu)$ denotes the product of the remaining $N-1$ eigenvalues of $I - D_x f^S(0; 0, \eta, \nu)$. $\mathcal{P}(\eta, \nu)$ is C^{K-1} and $\mathcal{P}(0, 0) \neq 0$ since the algebraic multiplicity of the eigenvalue 1 of $M_S(0)$ is one. Let

$$\kappa = \mathcal{P}(0, 0),$$

then, using (70),

$$\begin{aligned}\det(I - D_x f^S(0; 0, \eta, \nu)) &= (-c_3\eta - c_4\nu + O(2))(\kappa + O(1)) \\ &= -c_3\kappa\eta - c_4\kappa\nu + O(2) .\end{aligned}$$

Using (42), (64) and (65) we arrive at

$$c_3 = -\frac{\check{\delta}}{\kappa t_d} , \quad c_4 = -\frac{\check{\delta}}{\kappa t_{(l-1)d}} .$$

- 5) When $\eta = \nu = 0$, the $\check{\mathcal{S}}$ -cycle has two points on the switching manifold and coincides with the $\hat{\mathcal{S}}$ -cycle. Both $\check{x}_0(\mu, 0, 0)$ and $\check{x}_d(\mu, 0, 0)$ are fixed points of f^S . Let $\lambda_1(\mu)$ and $\lambda_2(\mu)$ be the respective eigenvalues of $D_x f^S(\check{x}_0(\mu, 0, 0); \mu, 0, 0)$ and $D_x f^S(\check{x}_d(\mu, 0, 0); \mu, 0, 0)$, C^{K-1} dependent on μ with $\lambda_1(0) = \lambda_2(0) = 1$. As above, since $\check{s}_0(\mu, 0, 0) = 0$, from (69)

$$\lambda_1(\mu) = \frac{\partial s'}{\partial s}(\check{s}_0(\mu, 0, 0); \mu, 0, 0) = 1 + c_2\mu + O(\mu^2) ,$$

and then since $\check{s}_d(\mu, 0, 0) = t_d\mu + O(\mu^2)$,

$$\begin{aligned}\lambda_2(\mu) = \frac{\partial s'}{\partial s}(\check{s}_d(\mu, 0, 0); \mu, 0, 0) &= 1 - \frac{2c_2}{t_d}(t_d\mu + O(\mu^2)) + c_2\mu + O(\mu^2) \\ &= 1 - c_2\mu + O(\mu^2) .\end{aligned}$$

Again, as above,

$$\begin{aligned}\det(I - D_x f^S(\check{x}_0(\mu, 0, 0); \mu, 0, 0)) &= -c_2\kappa\mu + O(\mu^2) , \\ \text{and } \det(I - D_x f^S(\check{x}_d(\mu, 0, 0); \mu, 0, 0)) &= c_2\kappa\mu + O(\mu^2) .\end{aligned}$$

But, recall (36), so

$$c_2 = -\frac{k_0}{\kappa} ,$$

and by (54)

$$\tilde{k}_0 = -k_0 . \tag{71}$$

Substitution of (71) into (61) verifies (iii) of the lemma (using also (64) and (65)). It now only remains to demonstrate (iv) and (v) of the lemma.

We have shown that the restriction of f^S to W^c is

$$s'(s; \xi) = s + \frac{k_0}{\kappa t_d}s^2 - \frac{k_0}{\kappa}\mu s - \frac{\check{\delta}}{\kappa t_d}\eta s - \frac{\check{\delta}}{\kappa t_{(l-1)d}}\nu s + \frac{\check{\delta}}{\kappa}\mu\eta + O(3) . \tag{72}$$

We now look for saddle-node bifurcations of (72). Since $\frac{\partial s'}{\partial s}(0; 0) = 1$ and $\frac{\partial^2 s'}{\partial s^2}(0; 0) \neq 0$, the implicit function theorem implies that there exists a unique C^{K-2} function, ψ such that $\frac{\partial s'}{\partial s}(\psi(\xi); \xi) = 1$ for small ξ and

$$\psi(\xi) = \frac{t_d}{2}\mu + \frac{\check{\delta}}{2k_0}\eta + \frac{\check{\delta}t_d}{2k_0t_{(l-1)d}}\nu + O(2) . \tag{73}$$

Then saddle-node bifurcations occur when $s'(\psi(\xi); \xi) = \psi(\xi)$. Let

$$\Lambda(\xi) = -\frac{4k_0\kappa}{\check{\delta}^2 t_d} (s'(\psi(\xi); \xi) - \psi(\xi)) . \quad (74)$$

Substitution of (72) and (73) into (74) yields (37). To complete verification of (iv) of the lemma we formally show that (72) has a saddle-node bifurcation at $\Lambda(\xi) = 0$ whenever $\mu > 0$ by verifying that all nondegeneracy conditions of the saddle-node bifurcation theorem [33] are indeed satisfied:

- 1) by construction, $\frac{\partial s'}{\partial s}(\psi(\xi), \xi) = 1$ when $\Lambda(\xi) = 0$,
- 2) $\frac{\partial s'}{\partial \tilde{\nu}} = \frac{\check{\delta} t_d}{2\kappa} \mu + O(2) \neq 0$ when $\mu > 0$ verifying transversality (where $\tilde{\nu}$ is given in (40)),
- 3) $\frac{\partial^2 s'}{\partial s^2} = \frac{k_0}{\kappa t_d} + O(1) \neq 0$.

Step 4: Compute the intersections of $\Lambda = 0$ with $\eta = 0$ and $\nu = \phi_2(\mu, \eta)$ to obtain the functions ζ_1 and ζ_2 .

To determine where $\Lambda(\xi) = 0$ intersects $\eta = 0$ it is natural to look at $\Lambda(\mu, 0, \nu) = 0$, but this is insufficient for a derivation of $\zeta_1(\mu)$ because we may not apply the implicit function theorem to $\Lambda(\xi)$ since it contains no linear terms. Instead we use the fact that when $\eta = 0$, the $\check{\mathcal{S}}$ -cycle is also an \mathcal{S} -cycle. We have $\Lambda = 0$ when, in addition, this periodic solution has an associated multiplier of 1 as an \mathcal{S} -cycle. This occurs when (using (36), (42) and (64))

$$\det(I - D_x f^{\mathcal{S}}(\check{x}_0(\mu, 0, \nu); \mu, 0, \nu) = k_0 \mu + \frac{\check{\delta}}{t_{(l-1)d}} \nu + O(2) = 0 ,$$

Application of the implicit function theorem to the previous equation produces

$$\nu = \zeta_1(\mu) = -\frac{k_0 t_{(l-1)d}}{\check{\delta}} \mu + O(\mu^2) .$$

Moreover,

$$\Lambda(\mu, 0, \nu) = \frac{1}{t_{(l-1)d}^2} (\nu - \zeta_1(\mu))^2 + o(|\nu - \zeta_1(\mu)|^2) ,$$

and so for $\mu > 0$, $\Lambda \geq 0$ on the ν -axis.

The curve $(\mu, \zeta_2(\mu), \phi_2(\mu, \zeta_2(\mu)))$ along which $\Lambda(\xi) = 0$ intersects the surface $\phi_2(\mu, \eta)$, is easily computed in a similar fashion. When $\mu > 0$, $\Lambda \geq 0$ along $\nu = \phi_2(\mu, \eta)$ and so $\Lambda \leq 0$ only when $\eta \leq 0$ and $\nu \geq \phi_2(\mu, \eta)$ and stated in the final part of the lemma. \square

Proof of Thm. 10. We begin by determining the region of admissibility of the $\check{\mathcal{S}}$ -cycle, $\{\check{x}_i\}$. From (28), $\check{x}_i(\xi) = \mu(y_i + O(1))$, thus since by assumption y_0 and y_{ld} are the only points of $\{y_i\}$ that lie on the switching manifold for small ξ with $\mu > 0$, here $\check{x}_i(\xi)$ lies on the same side of the switching manifold as y_i for each $i \neq 0, ld$. The n -cycle, $\{y_i\}$, is admissible by assumption (for $\mu > 0$), thus $\{\check{x}_i(\xi)\}$ is admissible exactly when $\check{s}_0, \check{s}_{ld} \geq 0$ (since $\check{\mathcal{S}}_0 = \check{\mathcal{S}}_{ld} = \mathbb{R}$). By

(30) and (31) $\check{s}_0, \check{s}_{ld} \geq 0$ when $\eta, \nu \geq 0$, therefore the $\check{\mathcal{S}}$ -cycle is admissible in Ψ_1 as stated in the theorem.

Similarly, for $\mu > 0$ the $\hat{\mathcal{S}}$ -cycle is admissible exactly when $\hat{s}_0, \hat{s}_{ld} \leq 0$ (since $\hat{\mathcal{S}}_0 = \hat{\mathcal{S}}_{ld} = \mathbf{L}$). By Lemma 9(ii), $\hat{s}_{ld}(\xi) = 0$ when $\eta = \phi_1(\mu, \nu)$. By (58), (65) and Lemma 9(i), $\frac{\partial \hat{s}_{ld}}{\partial \eta}(\xi) = -\frac{t_{(l-1)d}}{t_{-d}} + O(\xi)$ which is positive for small ξ , hence $\hat{s}_{ld} \leq 0$ for $\eta \leq \phi_1(\mu, \nu)$ when $\mu > 0$. Similarly by Lemma 9(iii), $\hat{s}_0(\xi) = 0$ when $\nu = \phi_2(\mu, \eta)$ and by (51), (64) and Lemma 9(i), $\frac{\partial \hat{s}_0}{\partial \nu}(\xi) = -\frac{t_d}{t_{(l+1)d}} + O(\xi)$ which is positive for small ξ , hence $\hat{s}_0 \leq 0$ for $\nu \leq \phi_2(\mu, \eta)$ when $\mu > 0$. Therefore the $\hat{\mathcal{S}}$ -cycle is admissible in Ψ_2 .

It remains to verify admissibility of \mathcal{S} -cycles. For the theorem in [10] this was straightforward since, if it existed, the \mathcal{S} -cycle was unique. The situation here is more complicated because there may be two coexisting, admissible \mathcal{S} -cycles. In the proof of Lemma 9 we determined the restriction of $f^{\mathcal{S}}$ to the center manifold through $(s; \xi) = (0; 0)$, (72). When $\mu > 0$ and $\Lambda(\xi) > 0$, locally the map (72) has two distinct fixed points, say, $s_{0,1}$ and $s_{0,2}$. We will denote the corresponding \mathcal{S} -cycles of (6) by $\{x_{i,1}\}$ and $\{x_{i,2}\}$ and assume $s_{0,1} \geq s_{0,2}$. For small ξ within $\{\xi \mid \mu > 0, \Lambda(\xi) > 0\}$, $s_{0,1}$ and $s_{0,2}$ are C^{K-1} functions of ξ .

On the surface $\Lambda(\xi) = 0$ the two solutions coincide (see (73)):

$$s_{0,1}(\xi) = s_{0,2}(\xi) = \psi(\xi), \text{ when } \Lambda(\xi) = 0.$$

At the intersection of $\Lambda(\xi) = 0$ and $\eta = 0$, namely $(\mu, 0, \zeta_1(\mu))$ (see Lemma 9(v)), $s_{0,1} = s_{0,2} = 0$. Thus by (73), on $\Lambda(\xi) = 0$, $s_{0,1} = s_{0,2} < 0$ when $\nu < \zeta_1(\mu)$ and $s_{0,1} = s_{0,2} > 0$ when $\nu > \zeta_1(\mu)$.

Now, for $\mu > 0$, $s_{0,1}$ and $s_{0,2}$ can only be zero if $\eta = 0$ because if $s = 0$ is a fixed point of (72) then the corresponding \mathcal{S} -cycle would also be an $\check{\mathcal{S}}$ -cycle which for $\mu > 0$ must be $\{\check{x}_i\}$, so then $\check{s}_0(\xi) = 0$ and by (30) we would necessarily have $\eta = 0$. Consequently one of $s_{0,1}$ and $s_{0,2}$ is zero when $\eta = 0$ and $s_{0,1}$ and $s_{0,2}$ are both nonzero when $\eta \neq 0$. Since we assume $s_{0,1} > s_{0,2}$ for $\Lambda(\xi) \neq 0$, when $\mu > 0$ and $\eta = 0$ we must have $s_{0,1} = 0$ when $\nu \leq \zeta_1(\mu)$ and $s_{0,2} = 0$ when $\nu \geq \zeta_1(\mu)$. Consequently $s_{0,1} < 0$ in $\Psi_2 \cup \Psi_3$ and $s_{0,2} < 0$ in $\Psi_1 \cup \Psi_2 \cup \Psi_3$.

Before we are able to perform a similar analysis of $s_{i,j}$ for $i \neq 0$, we find it necessary to first derive an expression for $s_{i,j}$ in terms of t_i and t_{d+i} . Recall that the center manifold, W^c , is given by (67) where $M_{\mathcal{S}}(0)v = v$ and $e_1^T v = 1$. When $\xi = 0$, y_0 and y_d are both fixed points of $h^{\mathcal{S}}$, thus $(I - M_{\mathcal{S}}(0))y_0 = P_{\mathcal{S}}(0)b(0) = (I - M_{\mathcal{S}}(0))y_d$ and so

$$(I - M_{\mathcal{S}}(0))(y_0 - y_d) = 0,$$

and since $y_0 \neq y_d$ (Lemma 7) and the eigenvalue 1 of the matrix $M_{\mathcal{S}}(0)$ has algebraic multiplicity one, $y_0 - y_d$ is a scalar multiple of v . Due to the specified vector scaling we have

$$v = \frac{1}{t_d}(y_d - y_0). \quad (75)$$

Combining (67) and (75) yields

$$x_{0,j}(\xi) = \left(\mu - \frac{s_{0,j}(\xi)}{t_d} \right) y_0 + \frac{s_{0,j}(\xi)}{t_d} y_d + O(2). \quad (76)$$

This may be generalized to an expression for $x_{i,j}(\xi)$ using $x_{i+1,j} = \mu b + A_{S_i} x_{i,j} + O(2)$ and $y_{i+1} = \mu b(0) + A_{S_i}(0)y_i$, from which we deduce

$$s_{i,j}(\xi) = \left(\mu - \frac{s_{0,j}(\xi)}{t_d} \right) t_i + \frac{s_{0,j}(\xi)}{t_d} t_{d+i} + O(2) , \quad (77)$$

and hence

$$s_{i,1}(\xi) - s_{i,2}(\xi) = -\frac{1}{t_d}(t_i - t_{d+i})(s_{0,1}(\xi) - s_{0,2}(\xi)) + O(2) .$$

Therefore for small $\xi > 0$ with $\mu > 0$ and $\Lambda(\xi) > 0$, $s_{i,1} > s_{i,2}$ if $t_i > t_{d+i}$ and $s_{i,1} < s_{i,2}$ if $t_i < t_{d+i}$ (because we assumed $s_{0,1} > s_{0,2}$).

Above we showed that when $\eta = \nu = 0$ and $\mu > 0$, $s_{0,1} = 0$ and $s_{0,2} < 0$. Thus here $s_{ld,1} = 0$ and $s_{ld,2} > 0$ and by Lemma 9, along $\eta = \phi_1(\mu, \nu)$, $s_{ld,1} = 0$ and $s_{ld,2} > 0$. From this it easily follows that $s_{ld,1} > 0$ in $\Psi_2 \cup \Psi_3$ and $s_{ld,2} > 0$ in $\Psi_1 \cup \Psi_2 \cup \Psi_3$. Similarly when $\nu = 0$ and $\mu > 0$, $s_{(l-1)d,1} < 0$ and $s_{(l-1)d,2} = 0$ and consequently $s_{(l-1)d,1} < 0$ in $\Psi_1 \cup \Psi_2 \cup \Psi_3$ and $s_{(l-1)d,2} < 0$ in $\Psi_1 \cup \Psi_3$. By analogous arguments, $s_{-d,1} > 0$ in $\Psi_1 \cup \Psi_2 \cup \Psi_3$ and $s_{-d,2} > 0$ in $\Psi_1 \cup \Psi_3$. By (77), for $i \neq 0, (l-1)d, ld, -d$, $s_{i,1}$ and $s_{i,2}$ have the desired sign for admissibility for small ξ with $\mu > 0$. The above statements show that $\{x_{i,1}\}$ is admissible in $\Psi_2 \cup \Psi_3$ and $\{x_{i,2}\}$ is admissible in $\Psi_1 \cup \Psi_3$ which completes the proof. \square

References

- [1] M. di Bernardo, C.J. Budd, A.R. Champneys, and P. Kowalczyk. *Piecewise-smooth Dynamical Systems. Theory and Applications*. Springer-Verlag, New York, 2008.
- [2] Z.T. Zhusubaliyev and E. Mosekilde. *Bifurcations and Chaos in Piecewise-Smooth Dynamical Systems*. World Scientific, Singapore, 2003.
- [3] S. Banerjee and G.C. Verghese, editors. *Nonlinear Phenomena in Power Electronics*. IEEE Press, New York, 2001.
- [4] R.I. Leine and H. Nijmeijer. *Dynamics and Bifurcations of Non-smooth Mechanical systems*, volume 18 of *Lecture Notes in Applied and Computational Mathematics*. Springer-Verlag, Berlin, 2004.
- [5] M. di Bernardo, P. Kowalczyk, and A. Nordmark. Bifurcations of dynamical systems with sliding: Derivation of normal-form mappings. *Phys. D*, 170:175–205, 2002.
- [6] M. di Bernardo, C.J. Budd, and A.R. Champneys. Corner collision implies border-collision bifurcation. *Phys. D*, 154:171–194, 2001.
- [7] Z.T. Zhusubaliyev and E. Mosekilde. Equilibrium-torus bifurcation in nonsmooth systems. *Phys. D*, 237:930–936, 2008.
- [8] T. Puu and I. Sushko, editors. *Business Cycle Dynamics: Models and Tools*. Springer-Verlag, New York, 2006.

- [9] M. di Bernardo, M.I. Feigin, S.J. Hogan, and M.E. Homer. Local analysis of C -bifurcations in n -dimensional piecewise-smooth dynamical systems. *Chaos Solitons Fractals*, 10(11):1881–1908, 1999.
- [10] D.J.W. Simpson and J.D. Meiss. Shrinking point bifurcations of resonance tongues for piecewise-smooth, continuous maps. *Nonlinearity*, 22(5):1123–1144, 2009.
- [11] A.B. Nordmark. Existence of periodic orbits in grazing bifurcations of impacting mechanical oscillators. *Nonlinearity*, 14:1517–1542, 2001.
- [12] D.J.W. Simpson and J.D. Meiss. Neimark-Sacker bifurcations in planar, piecewise-smooth, continuous maps. *SIAM J. Appl. Dyn. Sys.*, 7(3):795–824, 2008.
- [13] H.E. Nusse and J.A. Yorke. Border-collision bifurcations including “period two to period three” for piecewise smooth systems. *Phys. D*, 57:39–57, 1992.
- [14] Z.T. Zhusubaliyev, E. Mosekilde, S. Maity, S. Mohanan, and S. Banerjee. Border collision route to quasiperiodicity: Numerical investigation and experimental confirmation. *Chaos*, 16(2):023122, 2006.
- [15] I. Sushko and L. Gardini. Center bifurcation for two-dimensional border-collision normal form. *Int. J. Bifurcation Chaos*, 18(4):1029–1050, 2008.
- [16] I. Sushko, L. Gardini, and T. Puu. Tongues of periodicity in a family of two-dimensional discontinuous maps of real Möbius type. *Chaos Solitons Fractals*, 21:403–412, 2004.
- [17] P. Le Calvez. Rotation numbers in the infinite annulus. *Proc. Amer. Math. Soc.*, 129(11):3221–3230, 2001.
- [18] J. Franks. Periodic points and rotation numbers for area preserving diffeomorphisms of the plane. *Inst. Hautes Études Sci. Publ. Math.*, 71:105–120, 1990.
- [19] S. Schwartzman. Asymptotic cycles. *Annals of Math.*, 66(2):270–284, 1957.
- [20] D.J.W. Simpson. *Bifurcations in Piecewise-Smooth Continuous Systems*. World Scientific, Singapore, 2010.
- [21] W.-M. Yang and B.-L. Hao. How the Arnol’d tongues become sausages in a piecewise linear circle map. *Comm. Theoret. Phys.*, 8:1–15, 1987.
- [22] Z.T. Zhusubaliyev, E.A. Soukhoterlin, and E. Mosekilde. Quasi-periodicity and border-collision bifurcations in a DC-DC converter with pulsewidth modulation. *IEEE Trans. Circuits Systems I Fund. Theory Appl.*, 50(8):1047–1057, 2003.
- [23] M. di Bernardo, C.J. Budd, and A.R. Champneys. Normal form maps for grazing bifurcations in n -dimensional piecewise-smooth dynamical systems. *Phys. D*, 160:222–254, 2001.
- [24] S.K. Berberian. *Linear Algebra*. Oxford University Press, New York, 1992.

- [25] B. Kolman. *Elementary Linear Algebra*. Prentice Hall, Upper Saddle River, NJ, 1996.
- [26] N.B. Slater. The distribution of the integers N for which $\{\theta N\} < \phi$. *Proc. Cambridge Philos. Soc.*, 46:525–534, 1950.
- [27] N.B. Slater. Gaps and steps for the sequence $n\theta \bmod 1$. *Proc. Cambridge Philos. Soc.*, 63:1115–1123, 1967.
- [28] N.P. Fogg. *Substitutions in Dynamics, Arithmetics and Combinatorics*. Springer-Verlag, New York, 2002.
- [29] M. Morse and G.A. Hedlund. Symbolic dynamics II. Sturmian trajectories. *Am. J. Math.*, 62:1–42, 1940.
- [30] B. Hao and W. Zheng. *Applied Symbolic Dynamics and Chaos*. World Scientific, Singapore, 1998.
- [31] R.M. Siegel, C. Tresser, and G. Zettler. A decoding problem in dynamics and in number theory. *Chaos*, 2(4):473–493, 1992.
- [32] H.R. Dullin, J.D. Meiss, and D.G. Sterling. Symbolic codes for rotational orbits. *SIAM J. Appl. Dyn. Syst.*, 4(3):515–562, 2005.
- [33] J. Guckenheimer and P.J. Holmes. *Nonlinear Oscillations, Dynamical Systems, and Bifurcations of Vector Fields*. Springer-Verlag, New York, 1986.